SEDIMENT TEXTURAL CHARACTERISTICS OF THE RAVENGLASS ESTUARY; DEVELOPMENT OF A METHOD TO PREDICT PALAEO SUB-DEPOSITIONAL ENVIRONMENTS FROM ESTUARY CORE SAMPLES

Simon, N.[1], Worden, R.H.[1]*, Muhammed, D.D.[1], Utley, J.E.P.[1], Verhagen, I.T.E.[1], Griffiths, J.[1,2], Wooldridge. L.M.[1,3]

1. Department of Earth, Ocean and Ecological Sciences, University of Liverpool, Liverpool, L69 3GP, UK

2. BP Exploration, Chertsey Road, Sunbury-on-Thames, Middlesex, TW16 7LN, UK

3. BP Upstream Technology, Chertsey Road, Sunbury-on-Thames, Middlesex, TW16 7LN, UK

* Contact author: Richard Worden, r.worden@liverpool.ac.uk

Abstract

Here we present a new way to automatically classify the exact sub-environment of deposition of sediment from estuarine sediment cores. It can be challenging to define the exact sub-environment of deposition in core as sediment of a given appearance, or facies, can be found in multiple settings. This issue is important given that petrophysical, geomechanical and reservoir quality properties of sedimentary rocks are typically strongly influenced by the specific sub-environment of deposition. Here, using a ten-fold classification of depositional sub-environments, we have determined the sub-environments of 482 sample sites from the Ravenglass Estuary, in NW England, UK. We then analysed the textural characteristics of each of these samples using laser particle size analysis. A novel automatic textural classification scheme was then developed using a combination of visual discrimination of gravel and vegetated surfaces, principal component analysis and recursive portioning routine (RPART) in Rstudio. The new automatic textural classification scheme can resolve eight of the ten sub-environments of deposition: gravel beds, salt-marsh, mud flat, mixed flat, sand flat, tidal inlet, combined south foreshore/ebb tidal delta and combined tidal inlet/north foreshore. Our scheme cannot differentiate the spatially adjacent tidal inlet and north foreshore sediments as they are texturally identical. Similarly, the scheme cannot differentiate the spatially adjacent ebb tidal delta and southern foreshore sediments as they also are texturally identical. We have applied our surface-calibrated method to a 3 m Holocene core drilled through fine-grained surface sandflats into interbedded fine- and coarse-grained sands in the Ravenglass Estuary and successfully defined palaeo-environments of deposition. Our automatic approach to the definition of palaeo-environment of deposition approach supersedes a simple lithofacies-based approach for the Ravenglass Holocene core as we can define, cm-by-cm, how the exact estuarine sub-environments evolved over the last 10,000 years. This approach could also be applied to other modern estuaries and could be trialled for use with ancient and deeply buried sedimentary rocks deposited in equivalent marginal marine estuarine environment.

Keywords: Estuary, estuarine sediment, grain size, sorting, kurtosis, sediment classification, environmental interpretation, Holocene, sub-depositional environment, recursive partitioning, classification diagram

1. INTRODUCTION

Grain size is a fundamental property of sediments that affects sediment's entrainment, transport and deposition (Blott and Pye, 2001) and has a huge impact on sandstone petrophysical properties (Tiab and Donaldson, 2015). Using largely descriptive approaches based on core and outcrop, sedimentologists have, for many years, attempted to use a supervised learning approach and grain size variations to help determine sedimentary environments and the processes that were responsible for sediment deposition (Folk, 1966; Folk, 1968). However, grain size analysis of modern sediment has also been used to provide clues to the mode of transportation and the energy condition of the transporting medium; Table 1 lists numerous studies that have attempted to use textural characteristics to help establish overall environment of modern clastic sediments. For example, there have been attempts to use sediment textural characteristics to discriminate modern sedimentary environments such as beach, dune and river sands (Sevon, 1966), beach, coastal dune, inland dune, and fluvial sands (Moiola et al., 1974), beach, dune and aeolian environments (Biederman, 1962; Mason and Folk, 1958), dune, beach and river sands (Friedman, 1961). Greenwood (1969) used multivariate discriminant analysis on sediment properties (average grain size, sorting, skewness and kurtosis) to differentiate between wave lain sand and aeolian sand. Moiola and Spencer (1979) and Zubillaga and Edwards (2005) used discriminant analysis to differentiate between inland aeolian and coastal aeolian sands. Recently, there have been attempts to use modern data analysis approaches, such as principal component analysis (Flood et al., 2015), and data transforms (Purkait and Das Majumdar, 2014), to try to define statistically different depositional environments and facies from surface sediments and cores in modern environments. With several criteria available to discriminate environments of deposition and depositional processes, clastic sediment textural studies can provide evidence to help in the interpretation of clastic deposits of unknown origin (Visher, 1969). This approach provides the basis for the next step towards a truly genetic classification of sedimentary textures.

The petrographic characteristics of modern sands in their present environments can potentially be used to help determine depositional environment to interpret the genesis of ancient clastic deposits (Friedman, 1961). However, a possible problem in the analysis of grain size is that the same transport and depositional process can occur within a number of environments and the resulting textural response can be similar (Visher, 1969). To complicate things still further, sediment can be reworked and redeposited, there may post-depositional processes such as infiltration and there may be diagenetic processes (Worden and Burley, 2003) all of which may serve to obscure the relationship between depositional environment and sediment texture.

The ability to relate the textural characteristics of ancient sediments and sedimentary rocks to their specific sub-environment of deposition would be extremely useful in developing an understanding of sedimentary architecture. For example, interpretation of sedimentary sub-environment is the objective of core logging from oil and gas fields and sites planned for carbon capture and storage (Blackbourn, 2012). Assessment of the sum of a sediment's characteristics is used to design groups, known as facies, with a common set of attributes which are then assembled into facies associations that are, in turn, interpreted in terms of environment of deposition. By this approach, the interpretation of environment of deposition is indirect and sometimes struggles to result in interpretations of specific sub-environments. Areas of mixing in tidal-fluvial depositional environments, e.g., estuaries, present an interesting extra problem due to (1) multiple sources of sediment (2) the mobility of sediment and possible movement in and out of the estuary basin and (3) the relative susceptibility to relative sea-level changes and the consequent rapid changes from fluvial to estuarine to marine, and the reverse (Dalrymple and Choi, 2007).

Here we have developed a supervised learning approach that relates specific categories of depositional sub-environments to quantitative textural attributes. We have produced a classification diagram that can take grain size, and other attributes, from any sediment from the Ravenglass Estuary and automatically define the exact sub-environment of deposition. To achieve this, we have mapped the Ravenglass Estuary to define depositional sub-environments, collected 482 surface sediment samples from the range of sub-environments and defined texture using laser particle size analysis. The Ravenglass Estuary was chosen for this study because of its accessibility, its macro-tidally (7.55 m) influenced environment, and the wide range of estuarine sub-environments. The aim was to study textural attributes of each estuarine sub-environment and to determine if there are statistically significant differences between sediments from the various sub-depositional environments. This categorical classification approach to the Ravenglass Estuary sediments has been applied to a Holocene core drilled into the Ravenglass Estuary but it might serve as aid for the discrimination of sub-environments in ancient and deeply buried estuarine sediments. This approach was developed as the majority of a suite of Holocene cores, drilled during the overarching research project, were sand-rich and lacked diagnostic sedimentary structures. Many of the cores simply had metre after metre of relatively bland sand that we struggled to relate to the top-surface depositional environments.

This study addresses the following research questions, focused on the estuarine sediments of the Ravenglass Estuary (Fig. 1):

1. What depositional sub-environments and ranges of grain size, and other textural characteristics are present within the Ravenglass Estuary?

2. What controls the distribution of grain size, and other textural characteristics, in estuarine settings?

3. Is it possible to develop a classification scheme to enable prediction of depositional environment from sediment textural attributes?

4. Can grain size characteristics from Holocene, or older, sediment cores be used to predict or discriminate palaeo-estuarine environments?

2. STUDY SITE: RAVENGLASS ESTUARY

The Ravenglass Estuary is on the west coast of Cumbria, in north west England, United Kingdom. The estuary covers an area of about 5.6 km^2 and is a macro-tidal environment, of which 86% is intertidal, with a maximum tidal range of about 7.55 m (Bousher, 1999; Griffiths et al., 2018; Lloyd et al., 2013; Wooldridge et al., 2017b). Sediment in the Ravenglass Estuary is quartz-dominated but contains variable quantities of clay minerals (Daneshvar and Worden, 2018; Griffiths et al., 2019a; Griffiths et al., 2019b; Wooldridge et al., 2017a; Wooldridge et al., 2018; Wooldridge et al., 2019a) and so the estuary may be a good analogue for ancient and deeply buried sandstone petroleum reservoirs that contain chlorite-coated grains. For example, it may be an analogue for the tidally-influenced, shallow marine-deltaic Tilje Formation, Norway (Ehrenberg, 1993), the shallow marine to deltaic Lower Vicksburg Formation U.S.A. (Grigsby, 2001), and the braid-delta margin with foreshore and shoreface deposits of Garn Formation, Norway (Storvoll et al., 2002).

The Holocene sedimentary succession that has filled the Ravenglass Estuary sits on top of Devensian glacial till that is directly overlain either by peat beds or fluvial gravel beds. The glacial tills and the peat beds have distinctive clasts of the underlying bedrocks that have allowed lithostratigraphical divisions and ice-movement patterns to be discerned (Merritt and Auton, 2000). Changes in relative sea level during the Holocene were predominantly caused by glacio-eustatic sea-level change and spatially-variable glacio-isostatic crustal-rebound resulting from deglaciation (Lloyd et al., 2013; Merritt and Auton, 2000).

The Ravenglass Estuary has three rivers that feed the main estuary (Fig. 1): the Rivers Esk, Mite, and Irt. These rivers have average discharge rates of 4.2 m^3s^{-1} for the River Esk, 3.4 m^3s^{-1} for the River Irt, and 0.4 m^3s^{-1} for the River Mite (Bousher, 1999). In the lower Esk arm of the estuary (Fig. 1), the maximum discharge measured during the ebb tidal flow (estuary emptying) is slightly lower 4.99 m^3s^-

^{1} than the flood tidal flow (estuary filling) 5.41 m^3s^{-1}; the slightly lower ebb drainage was reported to be a result of the short length of the Ravenglass Estuary (Kelly et al., 1991).

The estuary is connected to the Irish Sea through a single, 500 m-wide tidal inlet (Fig. 1) that flows between two dune-topped barrier systems, the Drigg spit to the north and Eskmeals spit to the south (Wooldridge et al., 2017b). The estuary has previously been divided into discrete zones, which have been grouped into four categories based on the dominant physical processes active in each zone (Griffiths et al., 2018; Griffiths et al., 2019b) (and see Figs. 1 and 2): (1) the fluvial zones for the Esk, Mite, and Irt, which are freshwater dominated; (2) the brackish zones of the tide-dominated inner estuary parts of the Irt, Mite, and Esk; (3) the relatively mixed-energy (mainly tide- and wave-influenced) zone of the central basin with near-seawater salinity; and (4) the outer zone including the tidal channel (between the Drigg and Eskmeals barrier spits), foreshore and ebb-tidal delta, which are dominated by seawater with wave and/or tidal currents. The fluvial-to-estuarine Esk, Mite and Irt, their overbank deposits, the estuary central basin, the tidal inlet, the foreshore, and the ebb-tidal delta complex, together provide a complete fluvial to marine transect that has already been extensively studied in terms of depositional environments, compositional variation, detrital clay mineralogy, detrital clay coat abundance, and detrital clay coat mineralogy (Daneshvar and Worden, 2018; Griffiths et al., 2018; Griffiths et al., 2019a; Griffiths et al., 2019b; Verhagen et al., 2020; Wooldridge et al., 2017a; Wooldridge et al., 2017b; Wooldridge et al., 2018; Wooldridge et al., 2019a; Wooldridge et al., 2019b; Worden et al., 2020).

The Ravenglass Estuary has some of the morphological characteristics of a wave-dominated estuary, e.g., the presence of the Drigg and Eskmeal barrier spits and the mud-rich central basin (Griffiths et al., 2019b). Wave-dominated estuaries usually have a well-defined tripartite zonation; (i) a high energy, coarse-grained, outer-estuary, marine-dominated region, (ii) a low energy, fine-grained, central region with mixed marine- and fluvial-influences and (iii) a high energy, coarse-grained, fluvial-dominated, inner region (Bokuniewicz, 1995; Dalrymple et al., 1992). However, the Ravenglass Estuary does not wholly conform to this simple pattern as the central region is relatively sand-rich and the inner estuary is not especially coarse-grained (Griffiths et al., 2019b). This deviation from a simple model might plausibly be due to one or more of: (i) strong tidal currents that pass beyond the low-energy, central basin into the inner parts of the estuary, thus producing extensive tidal bars and tidal dunes complexes (Griffiths et al., 2019b), (ii) the Ravenglass Estuary is in the later stages of filling, as shown by the presence of a ebb-tidal delta, because ebb-tidal deltas have been reported to reduce the significance of the energy-minimum in the central part of an estuary (Posamentier and Walker, 2006), or (iii) as tidal energy increases relative to wave energy, marine-derived sand can be transported greater distances up-estuary, and the otherwise muddy central basin has been replaced by sandy tidal channels that are flanked by marshes (Dalrymple et al., 1992).

3. SAMPLES AND METHODS

To study the relationship between grain size distribution and depositional environment, sub-depositional estuarine environments were first defined by describing surface sediment characteristics, detailed ground surveys, aerial imagery, then surface sediment samples were collected (Fig. 1) for grain size analysis and finally the data were statistically modelled to examine links between sediment textural attributes and sub-depositional estuarine environments.

3.1. Field-Based Mapping and Sample Collection

Eleven sub-depositional environments were initially mapped and defined across the estuary, using aerial imagery and detailed surveys based on geomorphology of estuarine feature and sediment type (Fig. 2 and 3). These estuarine sub-environments are gravel beds (De1), tidal flats (De2-4), tidal bars (De5), tidal inlets (De6), backshore deposits (De7), foreshore deposits (NDe8) that were split between northern (NDe8), southern foreshore (SDe8), ebb-tidal delta deposits (De9) and salt marsh (De10). Using a classification scheme initially proposed by Brockamp and Zuther (2004), tidal flats (De2-4) have been split into three sub-divisions using laboratory-derived sand percentages into: mud flat (De2: 15 to 50% sand), mixed flat (De3: 50 to 90% sand) and sand flat (De4: 90 to 100% sand). The small area occupied by the backshore deposits (De7), the diminutive number of samples collected (two) and the low preservation-potential of this sub-environment, led us to remove this category from the classification scheme. We chose to exclude the dune-topped spit environments (nominally De11) from the scheme as they have negligible preservation-potential.

A total of 482 surface sediment samples (here defined as sediment from the top 2 cm) were collected from the estuary and nearby coast, at low tide, that provide a complete fluvial to marine transition (Fig. 1). As the estuary almost totally empties (86%) at low tide during which most channels are no more than 1 m deep, we had access to the entire estuary sediment surface, with the exception of the channel in the main tidal inlet. The sediment samples were placed in airtight plastic bags in the field and air-dried in the laboratory at the University of Liverpool for further study.

3.2. Grain size analysis using Laser Particles Size Analysis (LPSA) and GRADISTAT© software

Prior to automated grain size analysis, coarse materials and organic matter was removed. The Laser Particle Size Analyser (LPSA) only accepts particles up to 2 mm in size; therefore, samples containing, for example, pieces of shell, algae, wood, or grit, were passed through a 2 mm sieve. The relative mass of the > 2 mm fraction was noted, and the coarse fraction sample was retained. About 10 to 20 mL of loose sediment was transferred into a 100 mL Pyrex beaker. 30 mL of 6 % hydrogen peroxide was added to remove organic matter from each sample that contained organic matter. The samples were transferred onto a hotplate at 70 °C in a fume cupboard to aid digestion, and to evaporate the fluid. Each sample stood for at least one hour until all signs of oxidative reaction of organic matter had ceased. Clay- and organic-rich samples, in some cases, required additional hydrogen peroxide to ensure full removal of organic matter. Surfactant ethanol was added to minimise fizzing and so prevent sediment sample-loss. The organic digestion process was repeated until all signs of organic digestion had ceased. The sides of the Pyrex beaker were rinsed with a fine jet of distilled water to wash down any residue and guarantee preservation of the whole sediment sample. A small amount of Calgon was added to convert the dried sediment into a paste on a watch glass for mixing and homogenisation.

Laser particle size analysis was conducted on the entire dispersed sediment sample using a Beckman Coulter counter. The LPSA results were analysed using GRADISTAT© software (Blott and Pye, 2001) for the quantification of grain size distribution, mean grain size, grain size sorting, skewness, kurtosis, sand, silt and clay abundance, and the calculation of the proportions of specific sediment grain size fractions. Statistical parameters used in describing the grain-size sorting (σg) scale of the sediments are those proposed by Folk and Ward (1957), in which high values are indicative of poorly-sorted sediment. Grain-size sorting classes, as defined by the GRADISTAT© software (Blott and Pye, 2001) are as follows: 1.27–1.41 (well-sorted), 1.41–1.62 (moderately well-sorted), 1.62–2.0 (moderately-sorted), 2.0–4.0 (poorly-sorted), and 4–16 (very poorly-sorted).

3.3. Spatial Mapping

Spatial distribution maps of various textural attributes were plotted (Figs. 4-8) using an inverse distance weighted (IDW) interpolation function in ArcGIS to avoid the formation of valleys, ridges of extreme and unrepresentative values or spurious negative values (e.g., for grain size) (Watson and Philip, 1985). To ensure that the interpolated values on either side (marine versus estuarine) of the coastal barrier spits did not influence each other despite their relative spatial proximity, a polyline was drawn through the long axes of the Drigg and Eskmeals spits (Griffiths et al., 2018).

3.4. Holocene core

A 3 m sediment core was drilled through the Holocene succession in the tidal flats at Saltcoats in the Ravenglass Estuary under tender by Geotechnical Engineering Ltd (Fig. 9). This core was acquired using a Geotechnical light-weight "Pioneer" rotary rig since the on soft and environmentally sensitive surfaces heavy drilling rigs tend to have trouble safely traversing the terrain. The retrieved core was 12 cm in diameter, thus permitting extensive study. 1 m segments of core were retained in a semi-rigid plastic liners ready to enable transport back to the University of Liverpool for subsequent analysis. The sediment core segments were sliced and photographed wet and air-dried. Following this, detailed visual logging of each core segment was undertaken at a scale of 1:5. Facies associations were described in terms of grain size, colour, sedimentary structures, bed thickness, presence of roots and shell fragments, bioturbation index and type of bioturbation. The core was then subject to LPSA analysis using techniques described above, from samples taken every 5 cm.

3.5. Statistical Analysis

3.5.1. Multivariate statistical techniques (Principal Component Analysis)

Principal component analysis (PCA) was employed to look for clusters in the textural data. PCA is a statistical procedure that converts a set of observations of possibly correlated variables into a set of values of linearly uncorrelated variables, called principal components (PCs). This multivariate statistical technique has been used repeatedly to investigate variability in large data sets (Cheng et al., 2006; Dempster et al., 2013; Grunsky and Smee, 1999; Klovan, 1966). Each principal component represents a certain amount of variability in the data and the first two principal components (PC1 and PC2) typically account for most of the variation within the whole dataset (Reimann et al., 2008). Only principal components with eigenvalues > 1 are used when using PCA, as they account for most of the variance in the data.

Mean grain size, grain size sorting, skewness and kurtosis data (phi unit) from the Ravenglass Estuary were imported into MINITAB© 17 for PCA analysis. The PCA produces an analysis of the PCA (Table 2) and eigenvectors (Table 3), also referred to as principal component coefficients, or loadings, which describe the relative significance of a given component. The derived principal component values for each sample were then linked to their specific sub-environment categories. Cross-plots of the principal components, with data categorised by sub-environment, was employed (Fig. 10) to assess whether the approach could be employed to reveal the environment of deposition of the Ravenglass Estuary samples from unknown environments (e.g., from core samples).

3.5.2. ANOVA and Post Hoc Tests

As we will show, principal component analysis was helpful for discriminating the three types of tidal flat environments, but it lumped all the sand-dominated sub-depositional environments into one area of a cross plot of PC1 versus PC2. We therefore employed other approaches to establish whether textural data can be used to discriminate the sand-dominated sub-depositional environment. The statistical significance of textural differences between various pairs of sand-dominated sub-depositional environment was investigated using an Analysis of Variance (ANOVA) approach. Following ANOVA, post-hoc Tukey's honestly significant difference (HSD) test was also employed to highlight the numerical significance of differences between each sand-dominated sub-environment for each sediment textural characteristic. The difference between each pair for each textural attribute is defined as being significant if the "p" value is less than 0.025. ANOVA and post-hoc Tukey tests (Table 4) were performed in R statistical software (R Core Team, 2016).

3.5.3. Bivariate analysis, and boxplots and classification trees

Bivariate plots of sediment textural parameters for discrimination of sedimentary environments have been used by numerous authors for many years (Friedman, 1961; Friedman, 1979; Mason and Folk, 1958; Shepard et al., 1961). Plots of grain size sorting against skewness were used here to try to discern estuarine sub-environments (Fig. 11).

Boxplots, produced using ggplot2 in Rstudio (Wickham, 2016) were employed to visualise some of the key differences between environments of deposition in terms of sedimentary parameters (Fig. 12). Key value, indicated by the node points in the classification tree (see next) as a function of depositional environments, were added to the boxplots. The boxplots are best examined in conjunction with the output from the ANIOVA analysis (Table 4).

Classification of the environments of deposition (categorical data) was undertaken using the numerical descriptions of sedimentary texture (continuous data) that were used to characterise each environment and the Recursive Partitioning and Regression Tree (RPART) package (Therneau and Atkinson, 2019), that is available in R statistical software (R Core Team, 2016). Using RPART, a classification tree can be developed by the following process: first the single variable (e.g., grain size) is found which best splits the data into two groups. The data are separated at the decision node, and then this process is repeated separately to each sub-group with further decision nodes, and so on, repeatedly, until no more improvement can be made. RPART results in “leaf” (or terminal) nodes that represent the optimum final classification down that branch. Each leaf node lists the quantity of samples in that specific classification category (and all other categories), listed as a fractional quantity. The ideal is 100% certainty that the classification is correct, which is indicated by a fractional value of 1.00. If the fractional value is less than 1.00, this shows that the classification has some uncertainty. Uncertainty is the result of some samples from different categories (in this case environments of deposition) falling in overlapping parts of multi-dimensional classification space, i.e., there are some categories of depositional environments that have overlapping attributes, even when four or six dimensions are considered. In the Ravenglass Estuary, case we applied an initial RPART classification tree to the output from the Principal Component Analysis. which neatly separated each of De2, De3 and D4 from De5-De9 (for example see Fig. 10 for a bivariate slice through the data). We then applied a second RPART classification tree to mean grain size, sorting, skew, kurtosis, the medium sand fraction, and the silt fraction to optimally-separate De5, De6, NDe8, SDe8 and De9 (for example see Fig. 12 for how textural variables separate the data, one-by-one).

4. RESULTS

4.1. Depositional environments in the estuary

The distribution of sub-environments is illustrated in Figure 2 and the appearance of each sedimentary sub-environment is illustrated in Figure 3.

4.1.1. Inner estuary

The inner estuary is comprised of (i) gravel beds (De1), localised to the lower part of the Esk arm, and is dominated by a loose aggregate of rock fragments, (ii) localised vegetated salt marsh (De10) in the lower Esk arm, dominated by salt-tolerant plants, (iii) tidal bars (De5), which are sand bars in the intertidal zone that have their long axis (crest) oriented approximately parallel to the direction of the main current (Figs. 2 and 3).

4.1.2. Tidal flats

The central basin and parts of the inner estuary consist of sand flat (De4, 90-100% sand), (ii) mixed flat (De3, 50–90% sand), , (iii) mud flat (De2, 15–50% sand) and (iv) fully vegetated salt marsh (De10) (Figs. 2 and 3). The tidal flat sediment subdivision follows the scheme defined by Wooldridge et al. (2017b), which was adapted from the subdivisions initially proposed by Brockamp and Zuther (2004). The mud flat (De2) lies furthest away from the tidal inlet (De6) and is dominated by fallout of suspended sediment. The mixed flat (De3) lies between the sand flat and mud flat and is characterised by alternating bedload sedimentation and fallout from suspension. The sand-flat (De4) is an intertidal flat relatively close to the tidal inlet (De6) and is dominated by bedload transport of sand grade sediment. The salt marsh (De10) is a supratidal zone, or upper coastal intertidal zone, that is subjected to daily or occasional flooding by salt water or brackish water and is dominated by a dense stand of salt-tolerant plants.

4.1.3. Outer estuary

The outer estuary is comprised of (i) the tidal inlet (De6), (ii) the backshore (De7), (iii) the foreshore (De8), and (iv) the ebb-tidal delta (De9) (Figs. 2 and 3). The tidal inlet (De6) dissects Eskmeals and Drigg barrier spits and connects the open ocean and the coastal environments to the central and inner zones of the estuary (Fig. 2). The diminutive backshore area (De7) is tidally inundated only during spring tide and storm events and fringes the dunes sitting on the barrier spits. The foreshore (De8) is the section of beach between the backshore and the mean-low-water line. The foreshore splits between the northern foreshore (NDe8) and southern foreshore (SDe8) since the two areas have radically different grain sizes (Fig. 4). The ebb-tidal delta is exposed during spring tides (Fig. 2). The paucity of backshore (De7) samples and their negligible preservation potential have led us to exclude this environment from the classification scheme.

4.2. Estuarine sediment characteristics

The mapped distribution of grain size and sorting for the whole of the Ravenglass Estuary are presented in (Figs. 4 and 5). Skewness (Fig. 6) is defined as the asymmetry of a distribution from the mean of a data set (Brown, 1997). Kurtosis (Fig. 7) is defined as a measure of the relative peakedness or flatness of a distribution compared to the normal distribution (Brown, 1997).. The distribution patterns of the proportions of different sand fractions are presented in Figures 8A to 8E, and silt plus clay fraction distributions is presented in Figure 8F. The following text describes the distribution of sediment parameters in the sub-environments.

Inner and central estuary mud flats (De2) are poorly-sorted and very fine-grained (Figs. 2, 4, 5). Sediments in mixed flats (De3) are heterogeneous and poorly-sorted, containing both mud and sand. Within the inner and central estuary, there is a gradational change from the poorly-sorted, very fine to fine-grained mixed flat to moderately well-sorted to moderately-sorted, fine to medium-grained, sand flat (De4).

Tidal bars sediments (De5) are moderately well-sorted to well-sorted, and fine- to medium-grained (Figs. 2, 4, 5). The gravel beds in the Esk arm (De1) are moderately well-sorted and fine- to medium-grained. The salt marsh sediments in the Esk arm (De10) are poorly- to moderately-sorted, very fine- to medium-grained. Tidal inlet sediment (De6) is typically moderately well-sorted and medium-grained. Sediments in the southern foreshore (SDe8) and in ebb-tidal delta (De9) are finer grained and better sorted than the sediments within the northern foreshore (NDe8) (and the backshore sediment, De7). Grain sizes are most coarse in the tidal inlet and the northern foreshore nearest the mouth of the estuary.

Grain size and degree of sorting across the estuary tend to increase down channel and decrease toward the margin of the inner estuary and central basin (Figs. 4, 5). Kurtosis is heterogeneously distributed, and sediment skewness becomes positive upstream and in the central basin, and negative down channel (Figs. 6, 7). There is a heterogenous distribution of grain sizes in the estuary with a dominance of fine- and very fine-sand fractions in the inner estuary (De2, De3) and southern foreshore and ebb delta (SDe8 and De9) (Figs. 8D, E). The medium sand fraction is dominant in the tidal bars (De5), central basin sand flats (De4), tidal inlet (De6) and northern foreshore (NDe8) (Fig. 8C). Coarse-grained sand is most abundant in the tidal inlet (De6), the proximal part of the northern foreshore and in parts of the tidal bars (De5) (Fig. 8B). Very coarse sands are rare (Fig. 8A).

Grain size and kurtosis in Ravenglass Estuary are heterogeneous (Figs. 4 and 7). Ravenglass sediment in the main parts of the estuary tends to be negatively skewed (Fig. 6). The sediment evolves to being slightly positively skewed along the tidal inlet (De6) towards the open sea (Fig. 6). Towards the head of the arms of the estuary and in mud flats (De2) and mixed flats (De3), the sediment tends to become increasingly positively skewed. The sediment in the Ravenglass Estuary is well- to moderately well-sorted in the tidal inlet and foreshore sub-depositional environments (De6 and De8; Figs. 2 and 5). In the three inner arms of the Ravenglass Estuary (Irt, Mite and Esk), sedimentary deposits are poorly-sorted, e.g., where there are mud flat (De2) and mixed flat (De3) sub-depositional environments. In contrast the sediment is moderately well-sorted along the channel of the Irt inner arm, and tidal bars (De5) and sand flats (De4) of the inner Esk arm (Figs. 2 and 5).

The distribution of different grain size classes (Fig. 8) reveals that there is no simple correspondence between grain size and position in the estuary. Coarse sand is located along the tidal inlet (De6) and in the northern foreshore (NDe8) just to the north of the tidal inlet (De6, Fig. 8B). Medium sand is also located along the tidal inlet (De6), along most of the northern part of the foreshore (NDe8) and in tidal bars (De5) in the mid Irt and Esk estuaries (Fig. 8C). Fine sand has a distinctly different distribution than the medium sand and is concentrated in the southern foreshore (SDe8) and in the sand (De4), mixed (De3) and mud (De2) flats in the Irt and Esk Estuaries (Fig. 8D). Very fine sand, silt and clay tend to be concentrated in the upper parts of the Irt and Mite estuaries and in the margins of the Esk Estuary (Figs. 8E and F).

4.3. Holocene core

Based on visual description, it was possible to identify various grades of sand in the geotechnical core drilled into the sandflats near Saltcoats (Fig. 9). Even though the core was drilled into tidal flat sediment and much of the sediment is composed of fine-grained sand, there are coarse-grained intervals that would not automatically be expected to be associated with sandflats. There was a distinct lack of sedimentary structures typically associated with estuarine sediment (mud drapes, bi-directional current ripples, etc) and a lack of trace fossils that might have been diagnostic of specific sub-environments. Based on core description alone, it was not possible to unambiguously define the palaeo-depositional environments of the sand, even 1 m below the surface. The Holocene core was analysed using LPSA, which informed the final interpretation of the palaeo-environments of deposition. The grain size, sorting, skewness, kurtosis and medium sand fraction and mud fraction output data from the LPSA have been added to Figure 9.

5. DISCUSSION

5.1. Controls on sediment texture

Estuaries are variably influenced by tides (Dalrymple and Choi, 2007) and greater tidal influences will give rise to greater marine sediment flux into estuaries (Dalrymple et al., 1990; Dalrymple et al., 1992). Tidal activity mixes fresh-river and saline-marine waters and can cause flocculation and deposition of clay minerals (Allen, 1991). Tidal activity also re-suspends and transports sediments, creates bedforms, and scours channels (Wells, 1995).

5.2. Distribution of sediment grain sizes in the Ravenglass Estuary

Most of the coarse-grained sand is within, or near, to the tidal inlet (De6; Fig. 8B). This area is where the tidal flow velocities will be highest. The flood tide tends to have a higher flow rate than the ebb tide (Kelly et al., 1991), so it is understandable that coarse marine sand is preferentially flushed into the estuary instead of flushed out (Dalrymple and Choi, 2007; Dalrymple et al., 2012). We have added schematic net sediment transport vectors to Figure 8B to 8F to illustrate sand grain size movement patterns in the estuary. Note that the coarse sand tends to be absent in the central basin, probably as the flow rate will diminish when the flooding tide spills, or dissipates, into the wider basin from the narrower tidal inlet.

The medium-grained sand distribution shows a pattern similar to the coarse sand with medium sand being flushed into the tidal inlet (De6) part of the estuary from a marine source (NDe8) (Dalrymple and Choi, 2007; Dalrymple et al., 2012; Dalrymple et al., 1992) (Fig. 8C). However, there is also a substantial quantity of medium-grained sand associated with tidal bars (De5) in the Irt and Esk estuaries, separated from the medium sand in the tidal inlet, suggesting that some medium-grained sands have been transported into the estuary from the two main fluvial sources (Esk and Irt). It is possible that high fluvial discharge rates linked to storm events have been responsible for the influx of medium-grained fluvial sand (Dalrymple and Choi, 2007).

There is a strong contrast between the distributions of fine- and medium-grained sand (Figs. 8C and D). Much of the fine-grained sand seems to have been brought into the estuary from the two main fluvial sources (Rivers Irt and Esk) as fine sand has highest concentrations in Esk and Irt sand flats (De4) in the inner estuary. There is also a substantial proportion of fine sand in the tidal inlet (De6) but it preferentially sits along the south side, whereas the medium sand sits preferentially along the north side. This suggests that fine sand is transported from the fluvial environment, via the central basin and out into the marine setting along the southern side of the tidal inlet (De6), where it supplies sediment to the west of the Eskmeals spit on the southern foreshore (SDe8).

The very fine sand distribution (Fig. 8E) suggests either that very fine sand is fluvially-supplied nto the estuary or that the very fine sand tends not to be deposited in foreshore environments. The distribution of silt plus clay mimics the distribution of very fine-grained sand suggesting that clay and silt are predominantly derived from fluvial sources (Fig. 8F).

Sediment in the marine-dominated parts of Ravenglass Estuary, i.e., the tidal inlet (De6) and foreshore (SDe8 and NDe8) sub-depositional environments, tend to be negatively skewed with a relatively greater proportion of coarser than finer grains in the same sample (Figs. 2 and 6). Sediment in the central estuary and towards the margin of the inner estuary, i.e., mud flat (De2) and mixed flat (De3) sub-depositional environments, tends to be positively skewed with a relatively greater proportion of finer than coarser grains in the same sample (Figs. 2 and 6). This skewness pattern, together with the interpreted sediment transport patterns illustrated in Figure 8, suggests that the marine sediment supply is predominantly medium-grained and that the positive skew to finer sediment may be a consequence of minor mixing with the finer-grained, fluvial sediment (Fig. 6). Conversely, the fluvial sediment supply is predominantly fine-grained from the Esk and very fine-grained from the Irt, and that the negative skew in both to coarser sediment may be the result of minor mixing with the coarser-grained, marine sediment (Fig. 6).

Sorting is generally poor in the inner parts of Irt and Esk estuaries except for tidal bars (De5) and sand flats (De4) where the sediment is moderately well-sorted (Figs. 2 and 5). This suggests that the higher flow velocities required to create tidal bars and sand flats are responsible for more unimodal and more organised sediment. The tidal inlet (De6), much of the foreshore (SDe8, NDe8) and ebb delta (De9) are well-sorted or moderately well-sorted suggesting that the higher energy of the marine realm is better at developing unimodal and more organised sediment than the inner estuarine realm.

5.3. Discrimination of depositional sub-environments using sediment textural parameters

Textural parameters of sediments, e.g., mean grain size, sorting (standard deviation), kurtosis and skewness, have been used previously to attempt to discern environments of sediment deposition but most studies have focussed on sands from completely different depositional settings; e.g. fluvial and marine-paralic sands from the Texas River, USA (Rogers and Strong, 1959), dune, beach and aeolian sands from Mustang Island, Texas, USA (Mason and Folk, 1958), and foreshore, backshore and aeolian sands from Barnstaple Bay, UK (Greenwood, 1969). These approaches were predicated upon the assumption that sediment's quantitative textural parameters reflect depositional environment because these experience different modes of sediment transport and deposition. The published approaches (Table 1) were able to discern large-scale differences in environment of deposition (e.g., marine versus fluvial), but most of them were not designed to differentiate sub-environments in the same overall setting (e.g., within an estuary). The existing schemes and models listed in Table 1 do not consider complex mixing at the interface between marine and fluvial depositional environment. Here, we provide, for the first time, a classification scheme that relates grain size characteristics to estuarine depositional sub-environments.

The ability to identify the exact sub-environment of deposition in ancient and buried sandstones, e.g., from core samples, would enable a detailed understanding of how a given sand body accumulated and evolved laterally and stratigraphically. The ability to identify the exact sub-environment of deposition was a prime objective of this study of sediment from the core drilled through the Holocene succession at the Ravenglass Estuary. The aim was to enable the confident definition of the sub-environment of deposition rather than just to provide a general description of lithofacies.

5.3.1. Visual discrimination of gravel beds and vegetated salt marsh samples

For the first step in classification of sub-environments, it is important to realise that gravel beds (De1) and vegetated salt marsh (De10) Holocene surfaces can be identified visually from each sample without the need for any further sophisticated analysis of the material. Gravel beds have easily identified gravel and salt marsh samples have abundant roots. The first step in any classification therefore involved only visual classification. For clarity, we have excluded the dune-topped spits from the classification scheme because their preservation potential in estuarine sedimentary settings is negligible (Mountney and Thompson, 2002).

5.3.2. Principal component analysis discrimination of mud-, mixed and sand-flat samples from all remaining environments

The next stage in the classification involved principal component analysis of the textural data: grain size, sorting, skewness, kurtosis. Because we have not used the entire spectrum of grain size data, where the full spread of grain sizes must equal 100%, there was no need to apply any sort of data transformation before we undertook principal component analysis to avoid the problems of closed datasets (Park and Jang, 2020; Sahoo et al., 2020; Zhou et al., 1991). The first two principal components in the Ravenglass Estuary sample set have eigenvalues > 1 (Table 2) accounting for the vast majority (89.7 %) of the variance of the entire dataset. For the Ravenglass Estuary sediment texture dataset, PC1 accounts for 61.9 % of the variance and PC2 for 27.8% of the variance. Principal component-1 and principal component-2 from the grain size distribution and sub-environment dataset are illustrated in a bivariate plot (Fig. 10) which demonstrates that some groupings of sedimentary sub-environments can be easily discerned using this approach. Figure 10 differentiates mud flats (De2), mixed flats (De3) and sand flats (De4). However, the left-hand cluster of data-points shows that this approach struggles to differentiate the sand-dominated sub-depositional environments, i.e., tidal bar (De5), tidal inlet (De6), foreshore (De8) and ebb-tidal delta (De9) sub-environments. The overlap of sand-dominated sub-environments could possibly be a consequence of being deposited under broadly similar energy conditions leading to these sediments apparently having similar textural parameters. Some sand flat (De4) samples fall in the mass of other sand-dominated sub-depositional environments (De5-De9), and vice versa, suggesting that a two dimensional approach to prediction would probably have some degree of inaccuracy. Backshore sediment environments (De7) are not included in the statistical analysis as they are aerially restricted and very few samples were collected.

Previous attempts to differentiate sub-environments have employed a simpler bivariate approach comparing, for example, sorting and skewness (Friedman, 1961; Friedman, 1962; Friedman, 1979; Mason and Folk, 1958; Shepard et al., 1961). We have here mimicked this approach in Figure 11 which seems able to broadly differentiate mud flats (De2), mixed flats (De3), sand flats (De4), a discrete grouping of gravel beds (De1) and vegetated saltmarsh (De10), and the collection of sand-dominated environments (Fig. 11). The lower left-hand cluster of data-points in Figure 11 reveals that the sorting and skewness bivariate approach also struggles to differentiate the sand-dominated sub-depositional environments (De5 to De9).

5.3.3. ANOVA and Tukey HSD tests help discriminate tidal bars, tidal inlet, foreshore and ebb-tidal delta samples

To advance our ability to differentiate the sand-dominated tidal bar (De5), tidal inlet (De6), northern foreshore (NDe8), southern foreshore (SDe8) and ebb-tidal delta (De9) sub-depositional environments, we have employed quantitative textural data from the LPSA and subjected them to

Analysis of Variance (ANOVA) and post hoc Tukey Honestly Significant Different (HSD) statistical tests using R. The significance of the difference is defined by the derived “p” value where p greater than 0.1 represents an insignificant, p less than 0.05 represents a significant difference, p less than 0.01 represents a very significant difference, and p less than 0.001 represents an extremely significant difference. The pairs of sub-environments, the quantitative textural data used to assess the difference and the p values for differences that are at least significant are defined in Table 4. We have here avoided reporting non-significantly different pairs of environments.

The distribution maps in Figures 4 to 8 show that there are major differences in textural attributes across the estuary and these are spatially related to the origin of the sediment. The differences, and similarities, in quantitative textural data between the various sandy sub-environments, apparent using ANOVA and HSD tests can be visualised using boxplots, here plotted using ggplot2 in R (Wickham, 2016). We have here illustrated the mean grain size (Figs. 4), medium sand fraction (Figs. 8C), kurtosis (Fig. 7), skewness (Fig. 6), sorting (Fig. 5) and silt fraction (Fig. 8F) using boxplots (Figs 12A to F).

Mean grain size effectively discriminates tidal inlet (De6) and northern foreshore (NDe8) from tidal bar (De5), ebb delta (De9) and southern foreshore (SDe8) sediments (Fig. 12A, Table 4). The medium sand fraction (Fig. 12B, Table 4) can be used to discriminate southern foreshore (SDe8) from tidal bar (De5) and ebb delta (De9) sediments. Kurtosis values (Fig. 12C, Table 4) can be used to discriminate tidal bar (De5) and ebb delta (De9) sediments. Skewness can be used to differentiate tidal bar (De5) from tidal inlet (De6) and the two foreshore sub-environments (SDe8 and NDe8) but the differences are only marginally significant (Fig. 12D, Table 4). Sorting is generally not a good discriminator of estuarine sub-environments except that some northern foreshore (NDe8) sediments are especially poorly-sorted (Fig. 12E). Silt fraction values discriminate depositional environments De5 to De9 better than sorting, as well as being a key to differentiating De2-4 from De5-9 (Fig. 12F). Other differences and similarities are apparent from the collection of boxplots and the p values in Table 4. Based on the study of statistically significant differences between sub-environments and the cut-off values between them for the various textural parameters, it is looks as if it possible to discriminate between several of the five sand-dominated sub-environments.

5.3.4. Recursive partitioning and the development of the classification tree using RPART

The combination of visual analysis, and principal component analysis (PCA) followed by the machine learning approach of recursive partitioning in Rstudio (RPART) allows the construction of a method for the discrimination of eight out of the ten depositional sub-environments (Fig. 13). The RPART package (Therneau and Atkinson, 2019), available in R studio software (R Core Team, 2016), was applied to the PCA and sediment attribute data. Each decision node in Figure 13 splits the data using one data type. In each leaf (terminal) node, the classification (depositional environment) is first listed, followed by the quantity of samples in the training dataset in that specific classification category, listed as a fractional quantity. RPART can report the fraction of samples in each leaf node in each category but in Figure 13 we have simplified the classification tree by only reporting the fraction al amount of the dominant class to allow the diagram to be readable. Finally, RPART also reports the total percentage of the whole sample set that lies in each leaf node.

Using the PCA output data plus the fractional quantity of silt, the machine learning approach separated De2, De3 and De4 from the remaining environments, De5 to De9, (Fig. 13). Mudflats (De2) are nearly perfectly classified (note that the fraction of mudflats in that category is 0.98 in the training dataset). Mixed flats (De3) are also well differentiated (with a fraction of 0.84) but sand flats (De4) are less well differentiated, having a fractional quantity of 0.74 in the training dataset. This can be read as 74% probability of samples ending in this leaf node being sand flat samples.

Based on the grain size, sorting, skew, kurtosis, medium sand fraction and silt fraction, due to the great degree of similarity in the textural attributes of the tidal inlet (De6) and northern foreshore (NDe8) (Figs. 4, 5, 6, 7, 8, 11, 12), these environments were merged for the RPART classification. Similarly, the ebb-tidal delta (De9) and southern foreshore (SDe8) were merged. Grain size, sorting, skew, kurtosis, silt fraction and medium sand fraction data were run through RPART for De5, De6-

NDe8 and De9-SDe8. The classification diagram (Fig. 13) shows that there are different ways to achieve a classification of De5, De6-NDe8 and De9-SDe8, each with a different fractional degree of certainty ranging from a perfect 1.00 to a less good 0.62.

We have added the machine learning-derived decision node criteria to the boxplots in Figure 12 to show how the automated collective analysis of six variables translates into the critical values in terms of the single variables. For example, a grain size of greater than 306 μm is one of the main ways of defining the combined tidal inlet and northern foreshore (De6-NDe8) (Fig. 12A).

This proposed method, calibrated using surface sediments from known estuarine sub-environments, can be used to interpret grain size distribution data from cores from the Holocene succession at the Ravenglass Estuary, it could be possibly applied to other estuaries that have similar geomorphological histories and potentially it could be used to interpret the exact sub-environments of cores from ancient and deeply buried sandstones.

5.4. Application of the classification method to the Holocene core

Using the classification (decision tree) diagram in Figure 13, based on visual inspection, principal component analysis and the recursive partitioning routine RPART, we have been able to uniquely discriminate mudflat, mixed-flat and sandflat sub-environments throughout most of the core (Figs. 9, 14B). The base of the succession, from 300 cm to about 235 cm, is composed of interbedded mixed flat (De3) and sand flat (De4) sediment. This is overlain by 10 cm of mud flat sediment (De2). From 225 to 215 cm, there is tidal inlet-northern foreshore sediment (De6-NDe8). From 215 up to about 150 cm, there is peat and glacial till, which are not here defined as estuarine sub-environments. From 150-130 cm, the sediment is classified into the combined tidal inlet-northern foreshore (De6-NDe8) category (Fig. 13). The top 130 cm represents a sand flat sub-environments (De4), which is the same as the present day depositional sub-environment at the surface. In Figure 14, the sediment that was either tidal inlet or northern foreshore sediment (De6-NDe8) beds is most likely tidal inlet sediment

(De6) because, at the present day, tidal inlet sediments juxtapose sand flat (De4) and mud flat (De2) sediments whereas foreshore sediments nowhere directly juxtapose sand flat sediment (Fig. 2).

The overall evolution of sediment in this core was from sand flat, via mixed flat to mud flat with evolving depositional environments leading to the tidal inlet migrating to this point in the estuary. This was followed by up to several meters of primary peat accumulation, assuming substantial compaction has affected the 60 cm of peat in the core (van Asselen et al., 2009), followed by a late glacial event. More tidal inlet sediment was then superseded by sandflats, presumably as the pattern of environments migrated towards the present-day coastline. The application of the discrimination diagram in Figure 13 to a modern core has allowed us to make a much finer interpretation of the sequence of estuarine depositional sub-environments (Fig. 14) than would have been possible based only on visual analysis and description of the relatively bland sand-rich core that has few of the expected estuarine sedimentary structures and is trace fossil-poor (e.g., Fig. 9).

6. CONCLUSIONS

1. This work is the first high-resolution study of grain size distribution as a function of sedimentary sub-environments in a modern marginal–shallow marine setting. This work was undertaken at the Ravenglass Estuary, NW England, United Kingdom.

2. Ten estuarine sub-environments, that are likely to be preserved in the sedimentary record, were defined, and mapped across the estuary; these are gravel bed, salt marsh, mud flat, mixed flat, sand flat, tidal bars, tidal inlet, northern-foreshore, southern foreshore, and ebb-tidal delta (Fig. 2).

3. Sediment at the surface of the Ravenglass Estuary was derived from both marine and fluvial sources. The marine sediment is coarse- to medium-grained and is dominant at the north side of the tidal inlet, just into the central basin and on the northern part of the foreshore. The fluvial sediment is fine- to very-fine-grained and is dominant in the inner arms of the estuary, on the south side of the

tidal inlet and on the southern side of the foreshore. Net sediment transport patterns in the estuary have been interpreted on this basis.

4. Grain size data from 482 surface sediment samples were used to create a classification diagram to facilitate the discrimination of depositional sub-environments through a combination of the careful mapping of sedimentary sub-environments, visual sample description, laser particle size analysis, principal component analysis, and a recursive partitioning classification model (RPART) produced in the Rstudio environment. The approach permits the identification of eight out of the ten estuarine sub-environments based solely on the sediment's textural characteristics. With this approach, we can identify whether the environment of deposition of a Ravenglass Estuary sample was gravel bed, salt marsh, mud flat, mixed flat, sand flat, tidal bars, southern foreshore-plus-ebb tidal delta, and tidal inlet plus northern-foreshore sediment.

5. The method developed in this study has been applied to a core drilled into a present-day sand flat, through the Holocene succession at Ravenglass. The application of the machine-learning-derived classification tree has uniquely identified a range of Holocene estuarine palaeo-sub-environments, at the core site, responsible for the accumulation of 3 m of sediment.

6. The approach developed here, using grain size distribution from the Ravenglass Estuary to discriminate depositional sub-environments, could potentially be used in other estuaries or possibly in ancient and deeply buried estuarine sedimentary rocks where textural characteristic may need to be defined by petrographic techniques if the rock is cemented.

Acknowledgements

We are grateful to Petroleum Technology Development Fund (PTDF) for funding this research. This work was undertaken and supported by the University of Liverpool, Chlorite Consortium research group including BP, Equinor, Petrobras, Woodside, Shell, Eni and Chevron.

REFERENCES

Allen, J.R.L., 1991. Fine sediment and its sources, Severn Estuary and inner Bristol Channel, southwest Britain. Sedimentary Geology, 75: 57-65.

Biederman, E.W., 1962. Distinction of shoreline environments in New Jersey. Journal of Sedimentary Research, 32(2): 181-200.

Blackbourn, G.A., 2012. Cores and core logging for geoscientists. Whittles Publishing, Dunbeath, UK, 160 pp.

Blott, S.J., Pye, K., 2001. GRADISTAT: a grain size distribution and statistics package for the analysis of unconsolidated sediments. Earth Surface Processes and Landforms, 26(11): 1237-1248.

Bokuniewicz, H., 1995. Sedimentary systems of coastal-plain estuaries, Developments in Sedimentology. Elsevier, pp. 49-67.

Bousher, A., 1999. Ravenglass Estuary: Basic characteristics and evaluation of restoration options, Westlakes Scientific Consulting Ltd, Moor Row.

Brockamp, O., Zuther, M., 2004. Changes in clay mineral content of tidal flat sediments resulting from dike construction along the Lower Saxony coast of the North Sea, Germany. Sedimentology, 51(3): 591-600.

Brown, J.D., 1997. Skewness and kurtosis. Shiken: JALT testing & evaluation SIG.

Cheng, Q., Jing, L., Panahi, A., 2006. Principal component analysis with optimum order sample correlation coefficient for image enhancement. International Journal of Remote Sensing, 27(16): 3387-3401.

Dalrymple, R.W., Choi, K., 2007. Morphologic and facies trends through the fluvial–marine transition in tide-dominated depositional systems: a schematic framework for environmental and sequence-stratigraphic interpretation. Earth-Science Reviews, 81(3-4): 135-174.

Dalrymple, R.W., Knight, R.J., Zaitlin, B.A., Middleton, G.V., 1990. Dynamics and facies model of a macrotidal sand-bar complex, Cobequid Bay Salmon River Estuary (Bay of Fundy). Sedimentology, 37(4): 577-612.

Dalrymple, R.W., Mackay, D.A., Ichaso, A., Choi, K.S., 2012. Processes, morphodynamics, and facies of tide-dominated estuaries, Principles of Tidal Sedimentology. Springer, pp. 79-107.

Dalrymple, R.W., Zaitlin, B.A., Boyd, R., 1992. Estuarine facies models - conceptual models and stratigraphic implications. Journal of Sedimentary Petrology, 62(6): 1130-1146.

Daneshvar, E., Worden, R.H., 2018. Feldspar alteration and Fe minerals: origin, distribution and implications for sandstone reservoir quality in estuarine sediments. In: P.J. Armitage et al. (Eds.), Reservoir Quality of Clastic and Carbonate Rocks: Analysis, Modelling and Prediction. Geological Society Special Publication, pp. 123-139.

Dempster, M., Dunlop, P., Scheib, A., Cooper, M., 2013. Principal component analysis of the geochemistry of soil developed on till in Northern Ireland. Journal of Maps(3): 373.

Ehrenberg, S.N., 1993. Preservation of anomalously high-porosity in deeply buried sandstones by grain coating chlorite - examples from the Norwegian continental shelf. American Association of Petroleum Geologists Bulletin, 77(7): 1260-1286.

Flood, R.P., Orford, J.D., McKinley, J.M., Roberson, S., 2015. Effective grain size distribution analysis for interpretation of tidal–deltaic facies: West Bengal Sundarbans. Sedimentary geology, 318: 58-74.

Folk, R.L., 1966. A review of grain-size parameters. Sedimentology, 6: 73-93.

Folk, R.L., 1968. Petrology of sedimentary rocks, Austin, Texas: Hemphill.

Folk, R.L., Ward, W.C., 1957. Brazos river bar. A study in the significance of grain size parameters. Journal of Sedimentary Petrology, 27(1): 3-26.

Friedman, G.M., 1961. Distinction between dune, beach, and river sands from their textural characteristics. Journal of Sedimentary Research, 31(4): 514-529.

Friedman, G.M., 1962. On sorting, sorting coefficients, and the lognormality of the grain-size distribution of sandstones. Journal of Geology, 70: 737-753.

Friedman, G.M., 1979. Differences in size distributions of populations of particles among sands of various origins: addendum to IAS Presidential Address. Sedimentology, 26(6): 859-862.

Greenwood, B., 1969. Sediment parameters and environment discrimination: an application of multivariate statistics. Canadian Journal of Earth Sciences, 6(6): 1347-1358.

Griffiths, J., Worden, R.H., Wooldridge, L.J., Utley, J.E.P., Duller, R.A., 2018. Detrital clay coats, clay minerals, and pyrite: a modern shallow-core analogue for ancient and deeply buried estuarine sandstones. Journal of Sedimentary Research, 88(10): 1205-1237.

Griffiths, J., Worden, R.H., Wooldridge, L.J., Utley, J.E.P., Duller, R.A., 2019a. Compositional variation in modern estuarine sands: Predicting major controls on sandstone reservoir quality. American Association of Petroleum Geologists Bulletin, 103(4): 797-833.

Griffiths, J. et al., 2019b. Estuarine clay mineral distribution: Modern analogue for ancient sandstone reservoir quality prediction. Sedimentology, 66(6): 2011-2047.

Grigsby, J.D., 2001. Origin and growth mechanism of authigenic chlorite in sandstones of the lower Vicksburg Formation, South Texas. Journal of Sedimentary Research, 71(1): 27-36.

Grunsky, E.C., Smee, B.W., 1999. The differentiation of soil types and mineralization from multi-element geochemistry using multivariate methods and digital topography. Journal of Geochemical Exploration, 67: 287-299.

Kelly, M., Emptage, M., Mudge, S., Bradshaw, K., Hamilton-Taylor, J., 1991. The relationship between sediment and plutonium budgets in a small macrotidal estuary - Esk Estuary, Cumbria, UK. Journal of Environmental Radioactivity, 13(1): 55-74.

Klovan, J.E., 1966. The use of factor analysis in determining depositional environments from grain-size distributions. Journal of Sedimentary Research, 36(1): 115-125.

Lloyd, J.M., Zong, Y., Fish, P., Innes, J.B., 2013. Holocene and Late-glacial relative sea-level change in north-west England: implications for glacial isostatic adjustment models. Journal of Quaternary Science, 28(1): 59-70.

Mason, C.C., Folk, R.L., 1958. Differentiation of beach, dune, and aeolian flat environments by size analysis, Mustang Island, Texas. Journal of Sedimentary Research, 28(2): 211-226.

Merritt, J.W., Auton, C.A., 2000. An outline of the lithostratigraphy and depositional history of Quaternary deposits in the Sellafield district, west Cumbria. Proceedings of the Yorkshire Geological Society, 53: 129-154.

Moiola, R.J., Spencer, A.B., 1979. Differentiation of aeolian deposits by discriminant analysis. US Geological Survey Professional Paper(1052): 53.

Moiola, R.J., Spencer, A.B., Weiser, D., 1974. Differentiation of modern sand bodies by linear discriminant analysis. Gulf Coast Association of Geological Societies Transactions, 24: 321-326.

Mountney, N.P., Thompson, D.B., 2002. Stratigraphic evolution and preservation of aeolian dune and damp/wet interdune strata: an example from the Triassic Helsby Sandstone Formation, Cheshire Basin, UK. Sedimentology, 49(4): 805-833.

Park, N.W., Jang, D.H., 2020. Geostatistical Classification of Intertidal Surface Sediments Using Log-ratio Transformation and High-resolution Remote Sensing Imagery. Journal of Coastal Research: 157-165.

Posamentier, H.W., Walker, R.G. (Eds.), 2006. Facies models revisited, 84. SEPM Special Publication, Oklahoma.

Purkait, B., Das Majumdar, D., 2014. Distinguishing different sedimentary facies in a deltaic system. Sedimentary Geology, 308: 53-62.

R Core Team, 2016. R: A language and environment for statistical computing. R Foundation for Statistical Computing, Vienna, Austria.

Reimann, C., Filzmoser, P., Garrett, R.G., Dutter, R., 2008. Statistical Data Analysis Explained. John Wiley & Sons Ltd., Chichester, UK.

Rogers, J.J., Strong, C., 1959. Textural differences between two types of shoestring sands. Gulf Coast Association of Geological Societies Transactions, 9: 167-170.

Sahoo, P.K. et al., 2020. Regional-scale mapping for determining geochemical background values in soils of the Itacaiunas River Basin, Brazil: The use of compositional data analysis (CoDA). Geoderma, 376.

Sevon, W., 1966. Distinction of New Zealand beach, dune, and river sands by their grain size distribution characteristics. New Zealand Journal of Geology and Geophysics, 9: 212-223.

Shepard, F.P., Manar, R.Y., Young, R., 1961. Distinguishing between beach and dune sands. Journal of Sedimentary Research, 31(2): 196-214.

Storvoll, V., Bjørlykke, K., Karlsen, D., Saigal, G., 2002. Porosity preservation in reservoir sandstones due to grain-coating illite: a study of the Jurassic Garn Formation from the Kristin and Lavrans fields, offshore Mid-Norway. Marine and Petroleum Geology, 19(6): 767-781.

Therneau, T.M., Atkinson, E.J., 2019. An Introduction to Recursive Partitioning Using the RPART Routines. Comprehensive R Archive Network.

Tiab, D., Donaldson, E.C., 2015. Petrophysics, 4th edition. Elsevier, Amsterdam, 894 pp.

van Asselen, S., Stouthamer, E., van Asch, T.W.J., 2009. Effects of peat compaction on delta evolution: A review on processes, responses, measuring and modeling. Earth-Science Reviews, 92(1-2): 35-51.

Verhagen, I.T.E., Crisostomo-Figueroa, A., Utley, J.E.P., Worden, R.H., 2020. Abrasion of detrital grain-coating clays during sediment transport: Implications for diagenetic clay coats. Sedimentary Geology, 403: 105653.

Visher, G.S., 1969. Grain size distributions and depositional processes. Journal of Sedimentary Research, 39(3).

Watson, D.F., Philip, G.M., 1985. Comment on “a nonlinear empirical prescription for simultaneously interpolating and smoothing contours over an irregular grid” by F. Duggan. Computer Methods in Applied Mechanics and eEngineering, 50(2): 195-198.

Wells, J.T., 1995. Tide-dominated estuaries and tidal rivers, Developments in Sedimentology. Elsevier, pp. 179-205.

Wickham, H., 2016. ggplot2: Elegant graphics for data analysis. Use R! Springer, Switzerland, 226 pp.

Wooldridge, L.J., Worden, R.H., Griffiths, J., Thompson, A., Chung, P., 2017a. Biofilm origin of clay-coated sand grains. Geology, 45(10): 875-878.

Wooldridge, L.J., Worden, R.H., Griffiths, J., Utley, J.E.P., 2017b. Clay-coated sand grains in petroleum reservoirs: Understanding their distribution via a modern analogue. Journal of Sedimentary Research, 87(4): 338-352.

Wooldridge, L.J., Worden, R.H., Griffiths, J., Utley, J.E.P., 2018. The origin of clay-coated sand grains and sediment heterogeneity in tidal flats. Sedimentary Geology, 373: 191-209.

Wooldridge, L.J., Worden, R.H., Griffiths, J., Utley, J.E.P., 2019a. Clay coat diversity in marginal marine sediments. Sedimentology, 66: 1118-1138.

Wooldridge, L.J., Worden, R.H., Griffiths, J., Utley, J.E.P., 2019b. How to quantify clay-coat grain coverage in modern and ancient sediments. Journal of Sedimentary Research, 89: 135-146.

Worden, R.H., Burley, S.D., 2003. Sandstone diagenesis: the evolution from sand to stone. In: S.D. Burley, R.H. Worden (Eds.), Sandstone diagenesis, recent and ancient. International Association of Sedimentologists Reprint Series, pp. 3-44.

Worden, R.H. et al., 2020. Chlorite in sandstones. Earth Science-Reviews, 204: 103105.

Zhou, D., Chen, H.Z., Lou, Y.L., 1991. The logratio approach to the classification of modern sediments and sedimentary environments in northern South China Sea. Mathematical Geology, 23(2): 157-165.

Zubillaga, J.J.K., Edwards, A.C., 2005. Grain size discrimination between sands of desert and coastal dunes from northwestern Mexico. Revista Mexicana de Ciencias Geológicas, 22(3): 383-390.

FIGURE CAPTIONS

Figure 1; Location map of the Ravenglass Estuary, north-west England with inset map of location of estuary in the UK. Surface sediment (<2 cm) sample sites highlighted by yellow dots. The geotechnical core location (Figures 9 and 14) is also marked for reference.

Figure 2; Distribution of depositional-environments in the Ravenglass Estuary. Depositional environments are labelled; De1, gravel-bed; De2, mud-flat; De3, mixed-flat; De4, sand-flat; De5, tidal bars and dunes; De6, tidal-inlet; De7, backshore; De8, foreshore (northern and southern areas); De9, ebb-tidal delta; and De10, salt marsh. Tidal flats have been sub-divided by lab-derived sand percentages into sand flat (90-100% sand), mixed (sand-mud) flat (50–90% sand), and mud flat (15–50% sand). The classification is modified from the scheme initially proposed by Brockamp and Zuther (2004).

Figure 3; (A) image revealing characteristics of depositional environment; each site image in part B marked by the large yellow numbers. (B) Compilation of surface photographs taken throughout the Ravenglass Estuary. 1 and 2) inner estuarine sand-flats with mud-drapes. 3) inner estuary flood-dominated tidal-bar. 4) central basin mud-flat. 5) central basin, highly-bioturbated (Arenicola marina), mixed-flat. 6) central-basin low amplitude dunes. 7) upper-foreshore/tidal-inlet wave-formed ripples. 8) tidal-inlet, migratory 3D dunes. 9) tidal-inlet upper-phase plane bed, proximal to the ebb-channel. 10) wind-blown, upper-foreshore sediment. 11) lower-foreshore wave-ripples, with subtle shell-debris lag deposits. 12) gravel-bed, exposed in the inner-Esk Estuary.

Figure 4; Grain size (µm unit) distribution in the Ravenglass Estuary. With units defined by GRADISTAT© software (Blott and Pye, 2001). Boundaries between different environments of deposition have been taken from Figure 2. Note that mean grain size decreases toward the margins of the inner estuary and central basin. Mean grain-size classes are labelled accordingly: silt; lower very fine sand (vfL); upper very fine sand (vfU); lower fine sand (fL); upper fine sand (fU); lower medium sand (mL); upper medium sand (mU); lower coarse sand (cL).

Figure 5; Sorting distribution in the Ravenglass Estuary, with units defined by GRADISTAT© software (Blott and Pye, 2001). Boundaries between different environments of deposition have been taken from Figure 2. Note that textural maturity decreases toward the margins of the inner estuary and central basin, sandy sub-environments in the marginal marine settings are moderately to well-sorted. Grain-size sorting classes are labelled accordingly: well-sorted (Ws); moderately well-sorted (MWs); moderately-sorted (Ms); and poorly-sorted (Ps).

Figure 6; Skewness of grain size distribution in the Ravenglass Estuary, where skewness refers to the distortion or asymmetry that deviates from a symmetrical bell curve, or normal distribution. Boundaries between different environments of deposition have been taken from Figure 2. Note that the sediments skewed positively upstream and central basin and skewed negatively down channel.

Figure 7; Kurtosis of the grain size distribution in the Ravenglass Estuary, where kurtosis is defined as a measure of the relative peakedness or flatness, or tail magnitude of a distribution compared to the normal distribution (Brown, 1997). Boundaries between different environments of deposition have been taken from Figure 2. A high kurtosis value means that there are more outsize grains than samples with a low kurtosis value. Kurtosis is heterogeneously distributed.

Figure 8; Mapped sand fraction distribution patterns in the Ravenglass Estuary, (A) Fraction of very coarse-grained sand, (B) Fraction of coarse-grained sand, (C) Fraction of medium-grained sand, (D) Fraction of fine-grained sand, and (E) Fraction of very fine-grained sand. (F) Fraction of all silt fractions plus clay. Boundaries between different environments of deposition have been taken from Figure 2 and added to part A.

Figure 9; Graphic log of the 3 m core drilled in the tidal flats adjacent to the central basin of the Ravenglass Estuary with illustration of the variation of grains size, sorting, skewness, kurtosis (µm unit), the medium sand fraction and the silt fraction, all derived from LPSA analysis.

Figure 10; Interpreted bivariate plot of multivariate Principal Component Analysis (PCA) from all 482 samples from the Ravenglass Estuary using grain size data (mean grain size, sorting, skewness and kurtosis, phi unit). The dominant principal components, PC1 and PC2, discriminate the loading score of each sample and groupings of sedimentary environments can be discerned. The collection of data points to the lower left of the diagram shows that multivariate analysis struggles to differentiate the sand-dominated sedimentary environments (De5-De9). Backshore (De7) sediment is not included in the final sub-environment classification as there were too few data points and there is negligible preservation potential.

Figure 11; Bivariate plot of sorting and skewness (phi unit) showing that different groups of sub-environments can be partly discriminated. The collection of data points to the lower left of the diagram shows that this bivariate analysis cannot differentiate the sand-dominated sedimentary environments (De5-De9). Backshore (De7) samples are not included in the final sub-environment classification as there were too few data from a small area of sediment that has negligible preservation potential.

Figure 12; Boxplots of textural attributes of the sand-dominated sub-environments that clustered together in Figures 10 and 11. Boxplots contain the median and upper and lower quartile ranges. Outliers are defined as > (or <) 1.5 times the interquartile range, above the upper and below the lower quartiles. (A) Grain size of the five sand-dominated sedimentary environments with the median value defined (and in Parts B to F). (B) Medium sand fraction. (C) Kurtosis. (D) Skewness. (E) Sorting. (F) Silt fraction with the number of samples (count) and the median value defined. This figure should be examined in conjunction with Table 4 to reveal the most important differentiators between sub environments. The critical values for parts A to F have been taken from the machine learning-derived decision nodes in Figure 13.

Figure 13; Discrimination diagram for the discrimination of depositional sub-environments, based on samples collected from the Ravenglass Estuary, developed through a combination of visual analysis (Fig. 3), differentiation of the principal component data and plus grain size, sorting, skew, kurtosis, medium sand fraction and silt fraction data (Figs. 10, 11, 12), using supervised classification and the recursive partitioning package, RPART (Therneau and Atkinson, 2019), available in R studio software (R Core Team, 2016). Each machine-learning-derived decision node splits the data using one data type. In each leaf (terminal) node, the classification (in this case, the depositional environment) is first listed. The second value is the quantity of samples in that specific classification category, listed as a fractional quantity; high fractional quantities show that the classification has a high degree of certainty. Finally, the third value that RPART reports in the leaf nodes is the total percentage of the whole sample set that lies in each leaf node. This approach separated De2, De3 and De4 from De5 to De9 using the PCA output data plus the fractional quantity of silt. De5, De6-NDe8 and De9-SDe8 were subjected to RPART classification based on grain size, sorting, skew, kurtosis, silt fraction and medium sand fraction data. The pairs De6-NDe8 and De9-SDe8 were merged during feature engineering as the classification approach proved to be incapable of differentiating them. Each leaf (terminal) node lists the fraction of the samples in that specific classification category as a fractional quantity. Uncertainty, visible by fractional values less than 1.00, is the result of some samples falling in overlapping parts of multi-dimensional classification space, i.e., there are some categories (of depositional environments) that have overlapping attributes, even when four or six dimensions are considered.

Figure 14. Schematic sedimentary log of central basin tidal flats deposits with application of the classification tree in Figure 13. A) Graphic log of a core from a sand flat in the central basin, near the hamlet of Saltcoats, with the sub-environments defined in the column to the right of the graphic log following application of the classification diagram (Fig. 13). B) Interpreted bivariate plot of replicated

multivariate Principal Component Analysis (PCA) of samples from Holocene cores across Ravenglass Estuary, PC1 and PC2 discriminating loading score of each sampled, Ravenglass Estuary grain size data (mean grain size, sorting, skewness and kurtosis, phi unit). The replicated PCA shows the colour coded of each sampled within different sub-depositional environments.

TABLE CAPTIONS

Table 1. Summary of previous work on discrimination of sedimentary environment from sediment textural characteristics

Table 2. Summary of the eigenanalysis and discrimination proportion of each principal component

Table 3. Summary of eigenvectors of each principal component

Table 4. Collation of some of the significance values resulting from the ANOVA analysis and post-hoc Honestly Significant Difference (HSD) tests for the characteristics of the sand-dominated sedimentary environments. We have excluded differences that are at best marginally significant (when $P < 0.1$). We have here listed significant difference when $P < 0.05$ (*), very significant differences when $P < 0.01$ (**), and extremely significant differences when $P < 0.001$ (***).

Figure 1

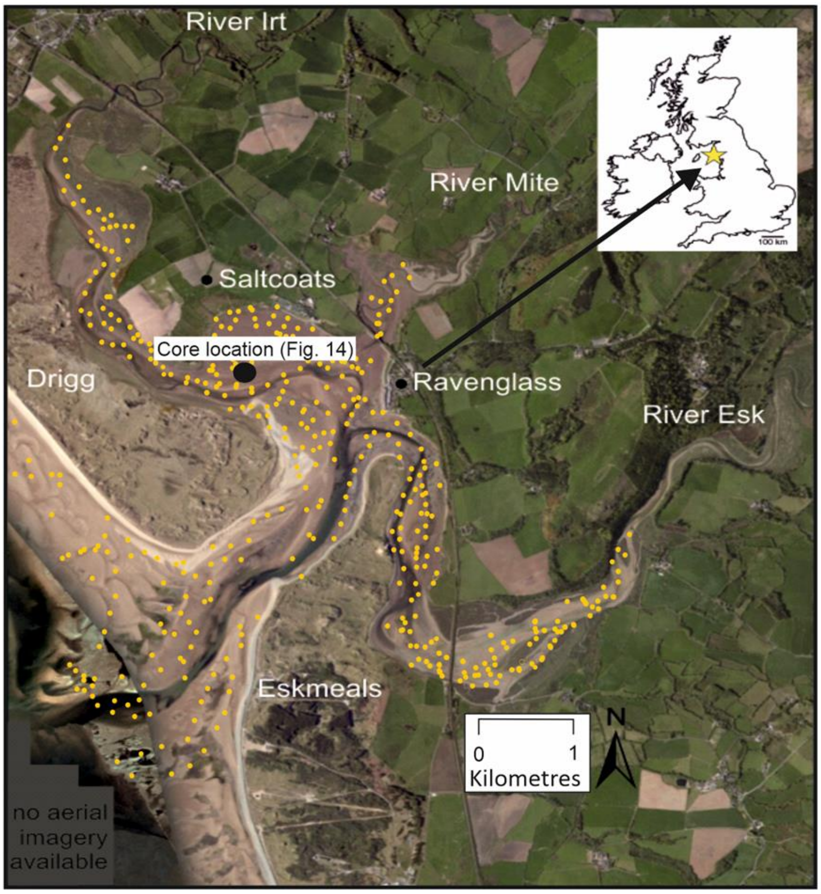

Figure 1; Location map of the Ravenglass Estuary, north-west England with inset map of location of estuary in the UK. Surface sediment (<2 cm) sample sites highlighted by yellow dots. The geotechnical core location (Figures 9 and 14) is also marked for reference.

Figure 2

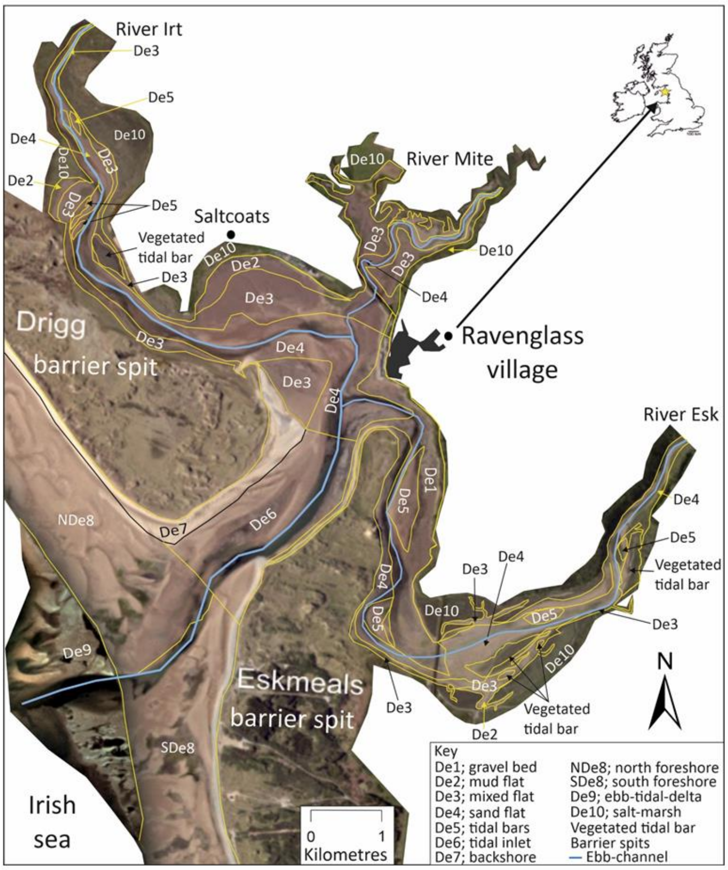

Figure 2; Distribution of depositional-environments in the Ravenglass Estuary. Depositional environments are labelled; De1, gravel-bed; De2, mud-flat; De3, mixed-flat; De4, sand-flat; De5, tidal bars and dunes; De6, tidal-inlet; De7, backshore; De8, foreshore (northern and southern areas); De9, ebb-tidal delta; and De10, salt marsh. Tidal flats have been sub-divided by lab-derived sand percentages into sand flat (90-100% sand), mixed (sand-mud) flat (50–90% sand), and mud flat (15–50% sand). The classification is modified from the scheme initially proposed by Brockamp and Zuther (2004).

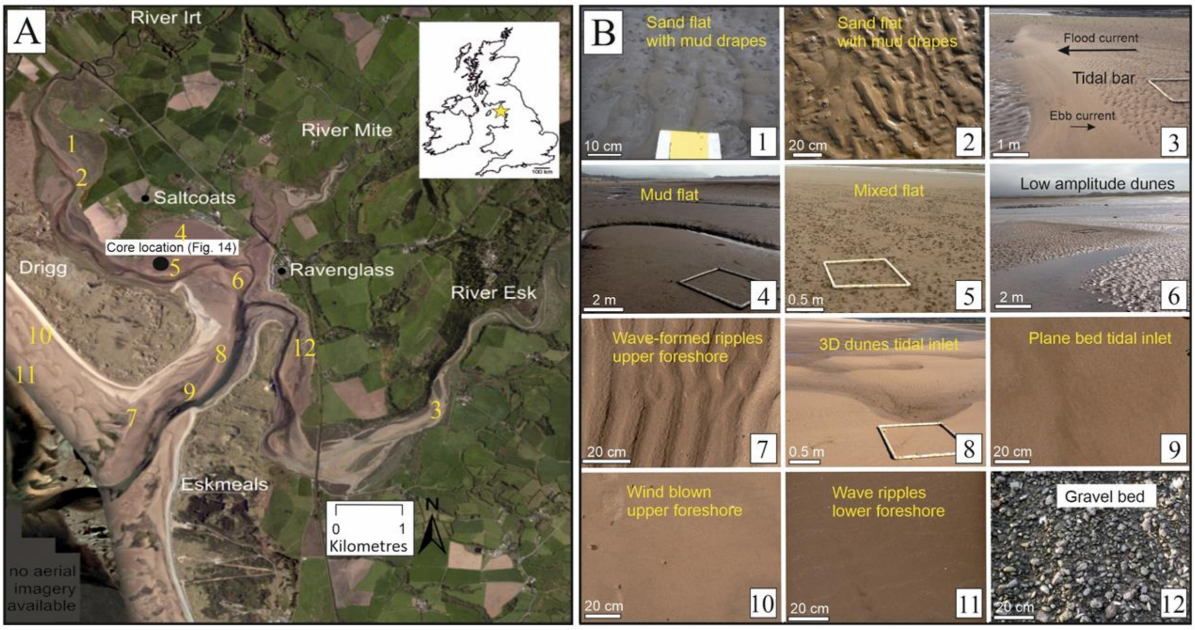

Figure 3

Figure 3; (A) image revealing characteristics of depositional environment; each site image in part B marked by the large yellow numbers. (B) Compilation of surface photographs taken throughout the Ravenglass Estuary. 1 and 2) inner estuarine sand-flats with mud-drapes. 3) inner estuary flood-dominated tidal-bar. 4) central basin mud-flat. 5) central basin, highly-bioturbated (Arenicola marina), mixed-flat. 6) central-basin low amplitude dunes. 7) upper-foreshore/tidal-inlet wave-formed ripples. 8) tidal-inlet, migratory 3D dunes. 9) tidal-inlet upper-phase plane bed, proximal to the ebb-channel. 10) wind-blown, upper-foreshore sediment. 11) lower-foreshore wave-ripples, with subtle shell-debris lag deposits. 12) gravel-bed, exposed in the inner-Esk Estuary.

Figure 4

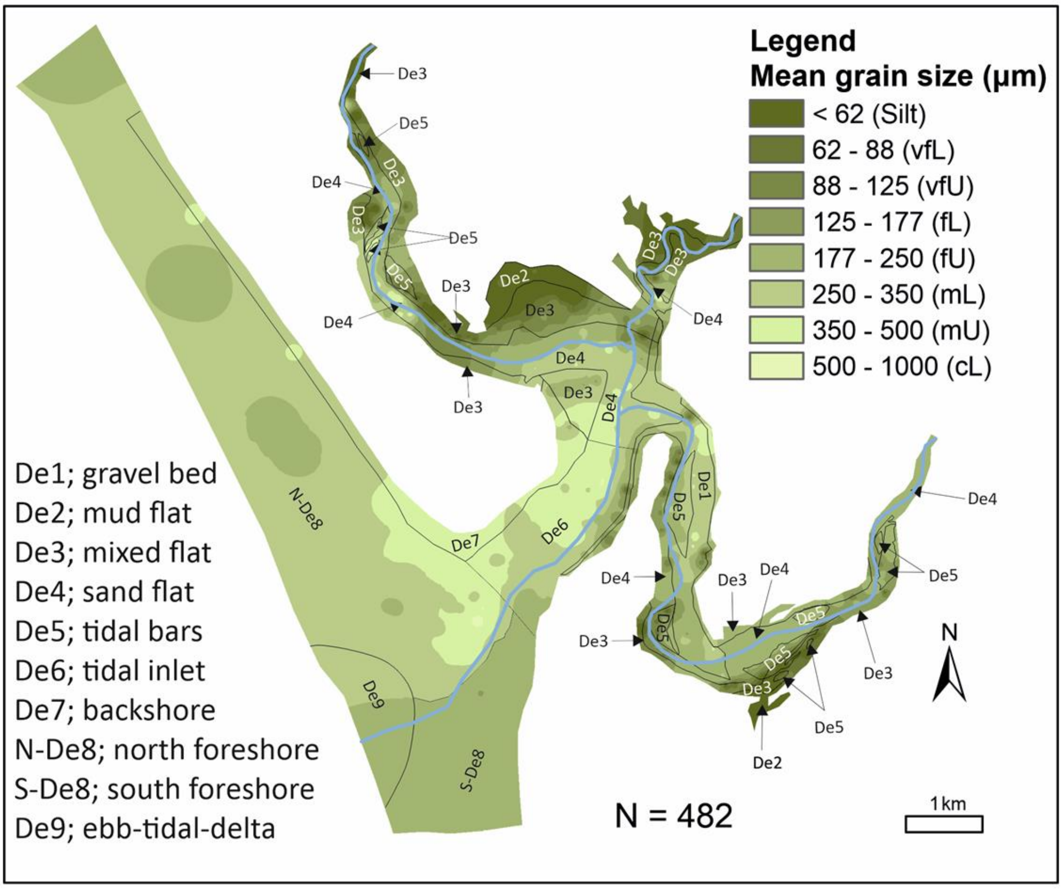

Figure 4; Grain size (µm unit) distribution in the Ravenglass Estuary. With units defined by GRADISTAT© software (Blott and Pye, 2001). Boundaries between different environments of deposition have been taken from Figure 2. Note that mean grain size decreases toward the margins of the inner estuary and central basin. Mean grain-size classes are labelled accordingly: silt; lower very fine sand (vfL); upper very fine sand (vfU); lower fine sand (fL); upper fine sand (fU); lower medium sand (mL); upper medium sand (mU); lower coarse sand (cL).

Figure 5

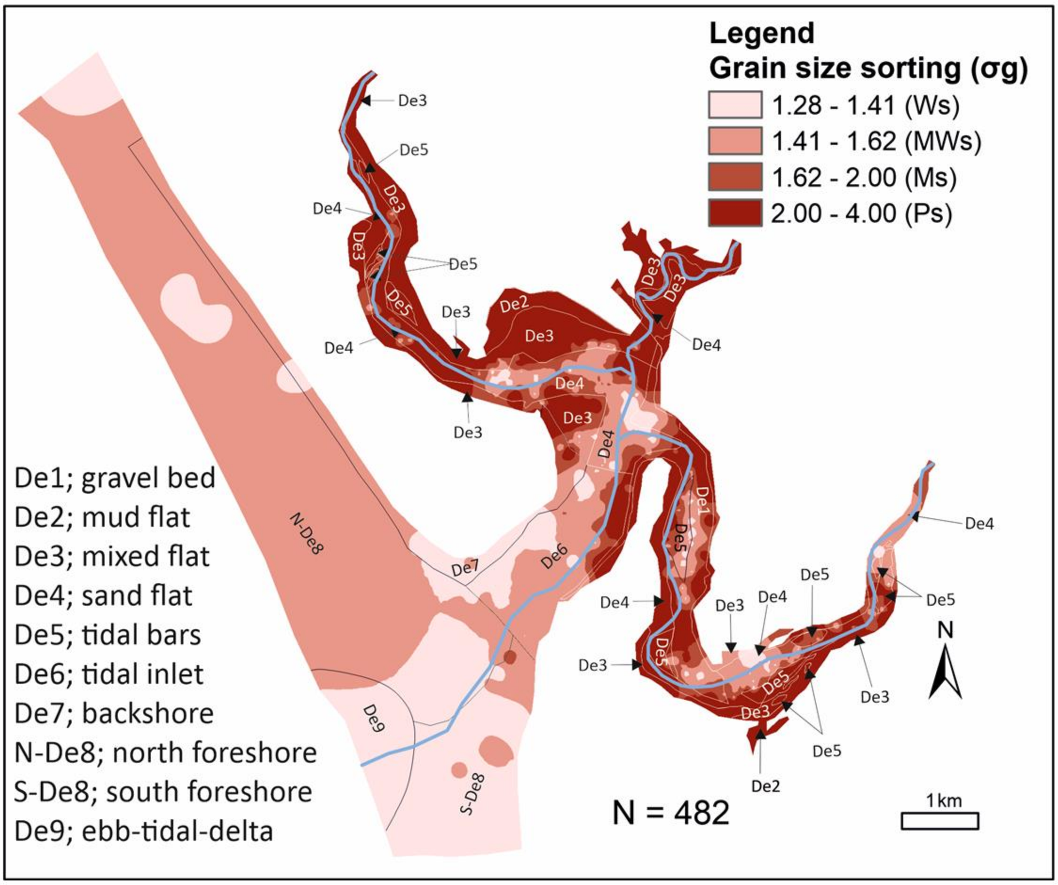

Figure 5; Sorting distribution in the Ravenglass Estuary, with units defined by GRADISTAT© software (Blott and Pye, 2001). Boundaries between different environments of deposition have been taken from Figure 2. Note that textural maturity decreases toward the margins of the inner estuary and central basin, sandy sub-environments in the marginal marine settings are moderately to well-sorted. Grain-size sorting classes are labelled accordingly: well-sorted (Ws); moderately well-sorted (MWs); moderately-sorted (Ms); and poorly-sorted (Ps).

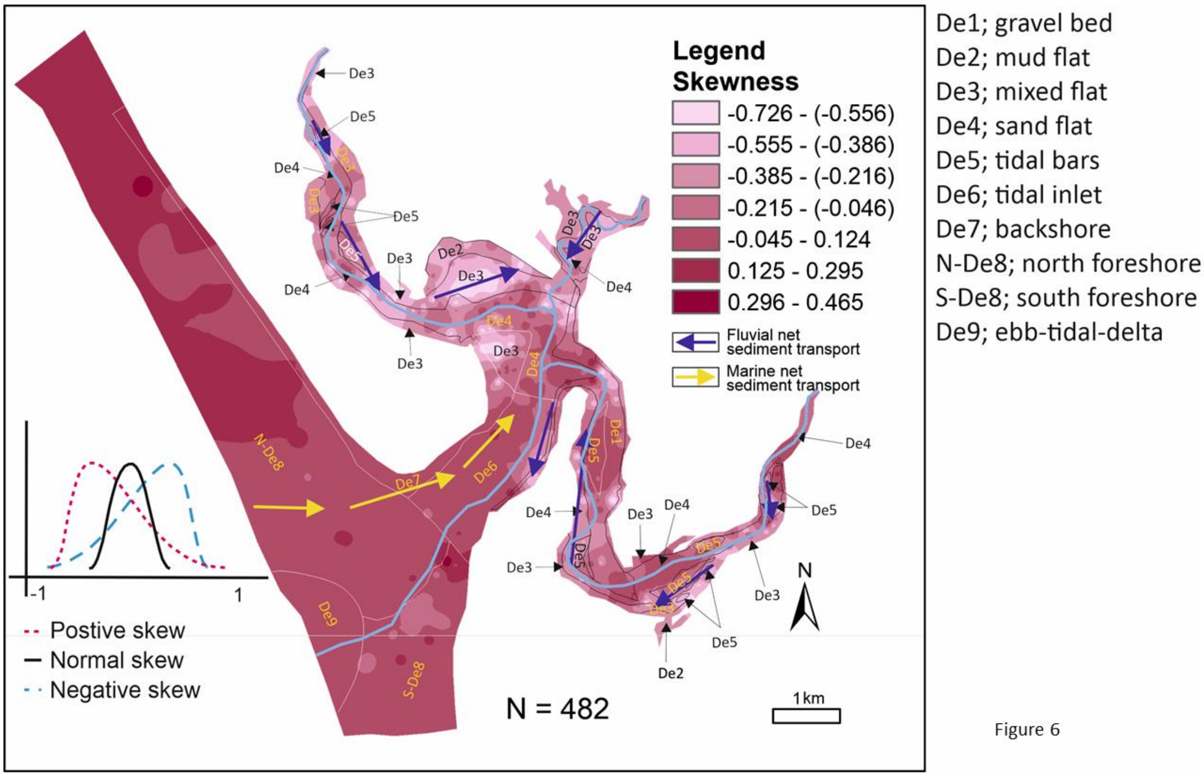

Figure 6; Skewness of grain size distribution in the Ravenglass Estuary, where skewness refers to the distortion or asymmetry that deviates from a symmetrical bell curve, or normal distribution. Boundaries between different environments of deposition have been taken from Figure 2. Note that the sediments skewed positively upstream and central basin and skewed negatively down channel.

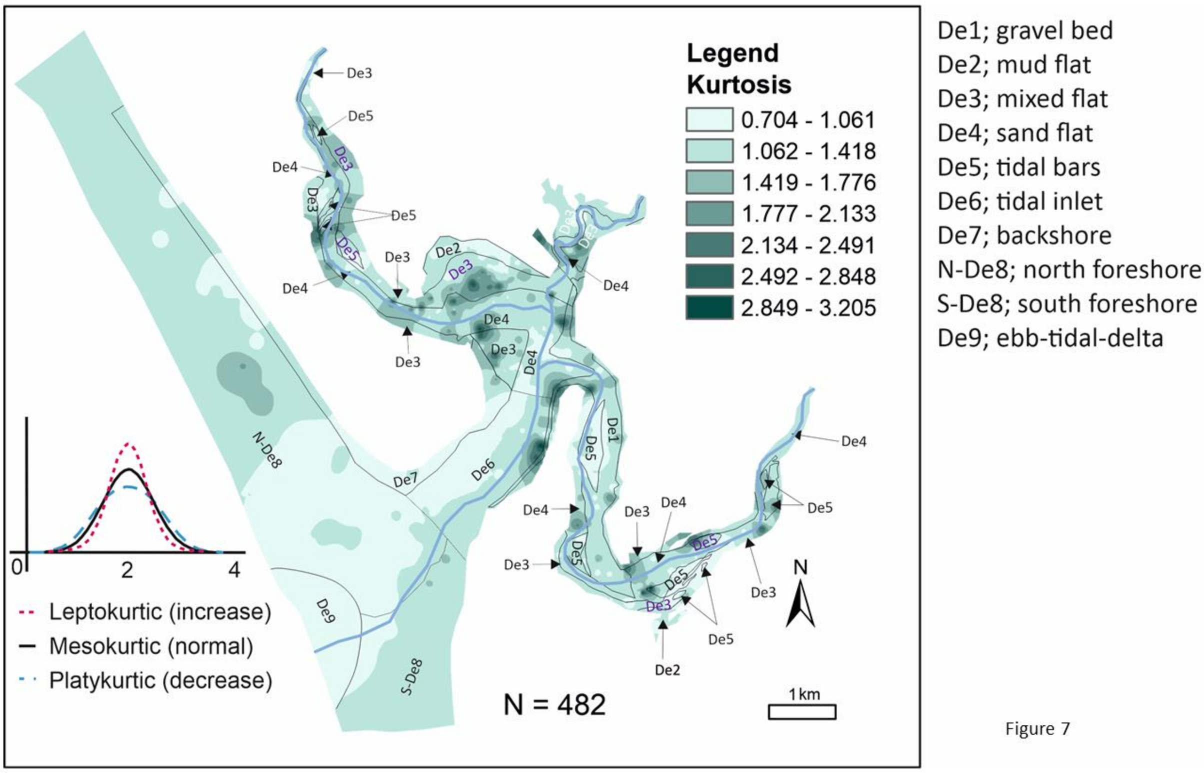

Figure 7; Kurtosis of the grain size distribution in the Ravenglass Estuary, where kurtosis is defined as a measure of the relative peakedness or flatness, or tail magnitude of a distribution compared to the normal distribution (Brown, 1997). Boundaries between different environments of deposition have been taken from Figure 2. A high kurtosis value means that there are more outsize grains than samples with a low kurtosis value. Kurtosis is heterogeneously distributed.

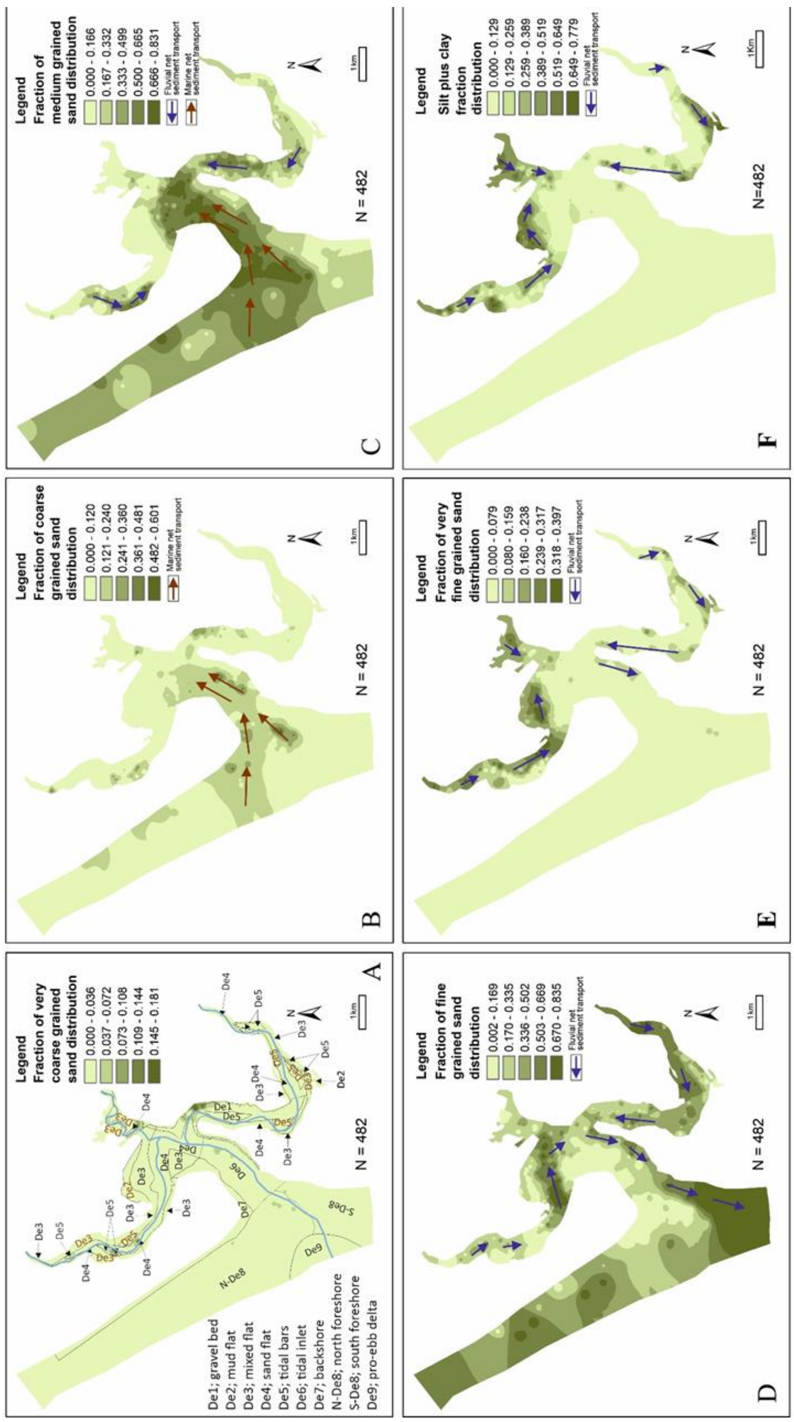

Figure 8 (please print this figure in landscape mode)

Figure 8; Mapped sand fraction distribution patterns in the Ravenglass Estuary, (A) Fraction of very coarse-grained sand, (B) Fraction of coarse-grained sand, (C) Fraction of medium-grained sand, (D) Fraction of fine-grained sand, and (E) Fraction of very fine-grained sand. (F) Fraction of all silt fractions plus clay. Boundaries between different environments of deposition have been taken from Figure 2 and added to part A.

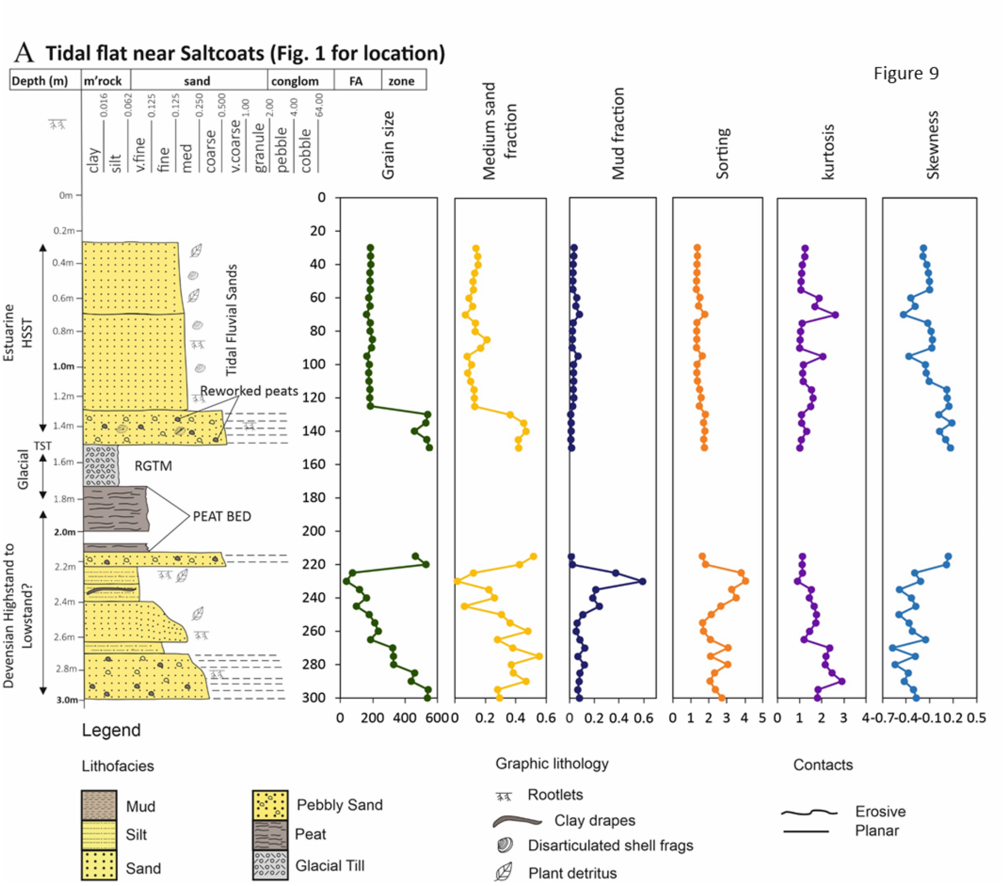

Figure 9; Graphic log of the 3 m core drilled in the tidal flats adjacent to the central basin of the Ravenglass Estuary with illustration of the variation of grains size, sorting, skewness, kurtosis (µm unit), the medium sand fraction and the silt fraction, all derived from LPSA analysis.

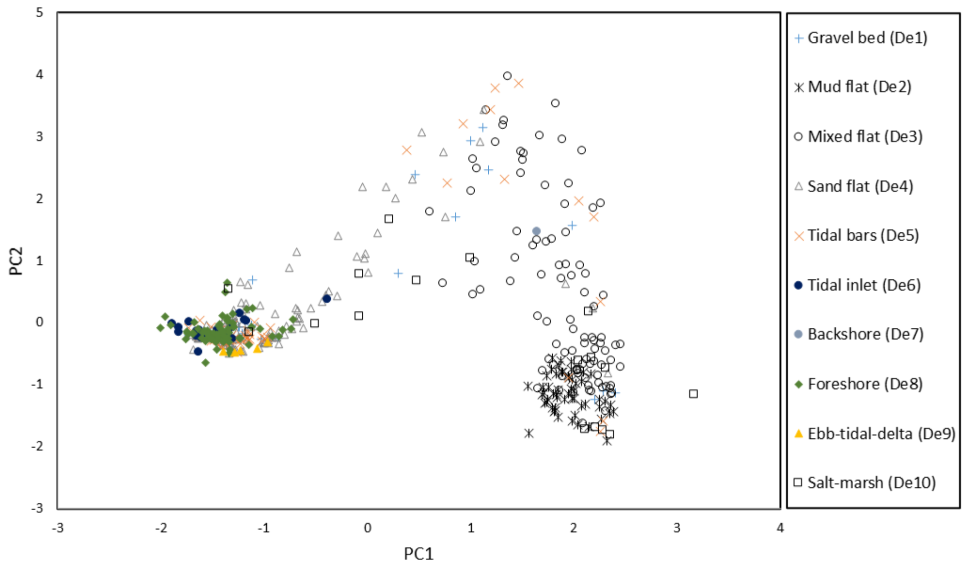

Figure 10

Figure 10; Interpreted bivariate plot of multivariate Principal Component Analysis (PCA) from all 482 samples from the Ravenglass Estuary using grain size data (mean grain size, sorting, skewness and kurtosis, phi unit). The dominant principal components, PC1 and PC2, discriminate the loading score of each sample and groupings of sedimentary environments can be discerned. The collection of data points to the lower left of the diagram shows that multivariate analysis struggles to differentiate the sand-dominated sedimentary environments (De5-De9). Backshore (De7) sediment is not included in the final sub-environment classification as there were too few data points and there is negligible preservation potential.

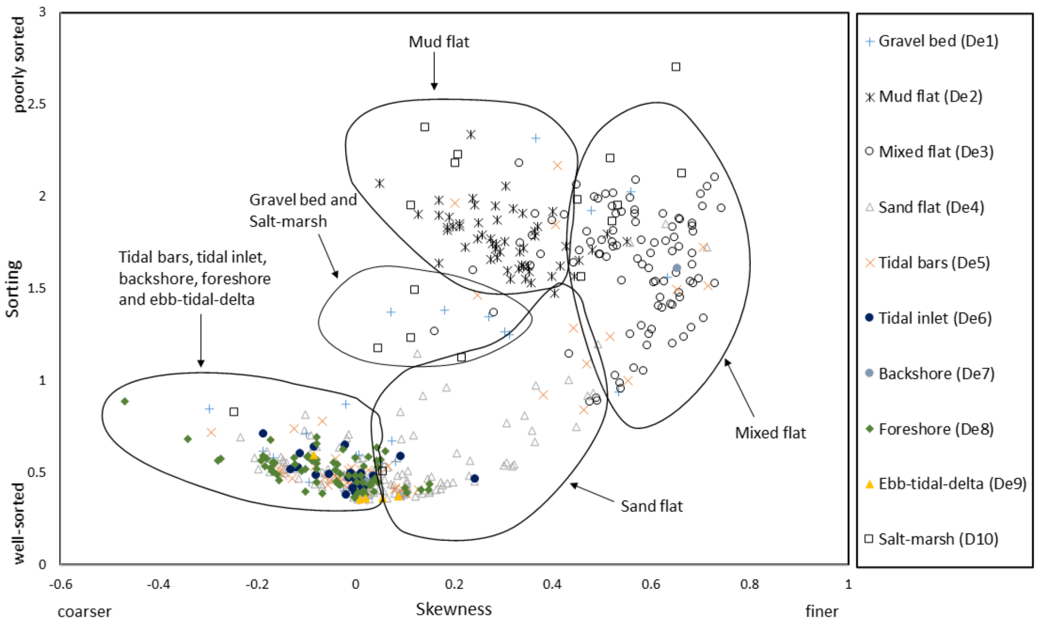

Figure 11

Figure 11; Bivariate plot of sorting and skewness (phi unit) showing that different groups of sub-environments can be partly discriminated. The collection of data points to the lower left of the diagram shows that this bivariate analysis cannot differentiate the sand-dominated sedimentary environments (De5-De9). Backshore (De7) samples are not included in the final sub-environment classification as there were too few data from a small area of sediment that has negligible preservation potential.

Figure 12

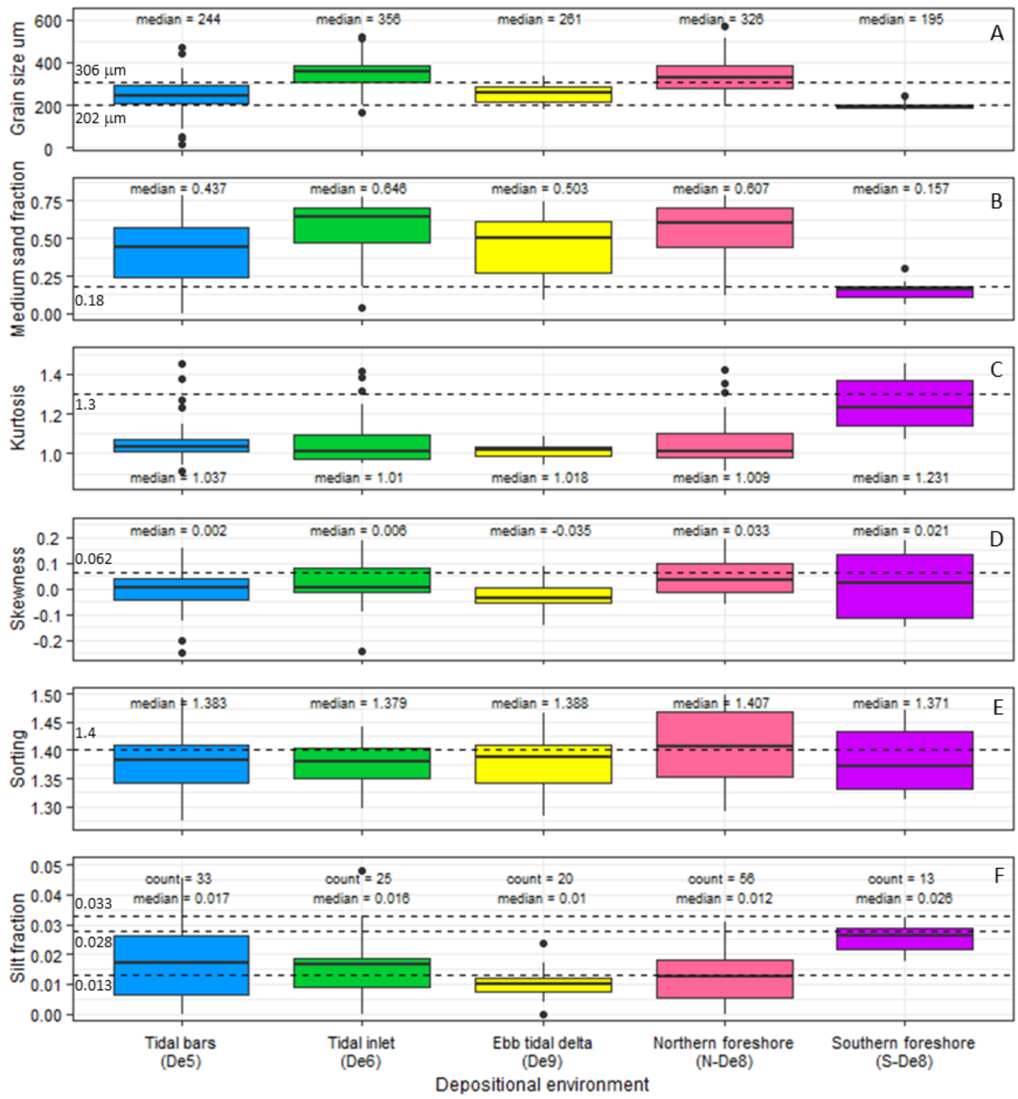

Figure 12; Boxplots of textural attributes of the sand-dominated sub-environments that clustered together in Figures 10 and 11. Boxplots contain the median and upper and lower quartile ranges. Outliers are defined as > (or <) 1.5 times the interquartile range, above the upper and below the lower quartiles. (A) Grain size of the five sand-dominated sedimentary environments with the median value defined (and in Parts B to F). (B) Medium sand fraction. (C) Kurtosis. (D) Skewness. (E) Sorting. (F) Silt fraction with the number of samples (count) and the median value defined. This figure should be examined in conjunction with Table 4 to reveal the most important differentiators between sub environments. The critical values for parts A to F have been taken from the machine learning-derived decision nodes in Figure 13.

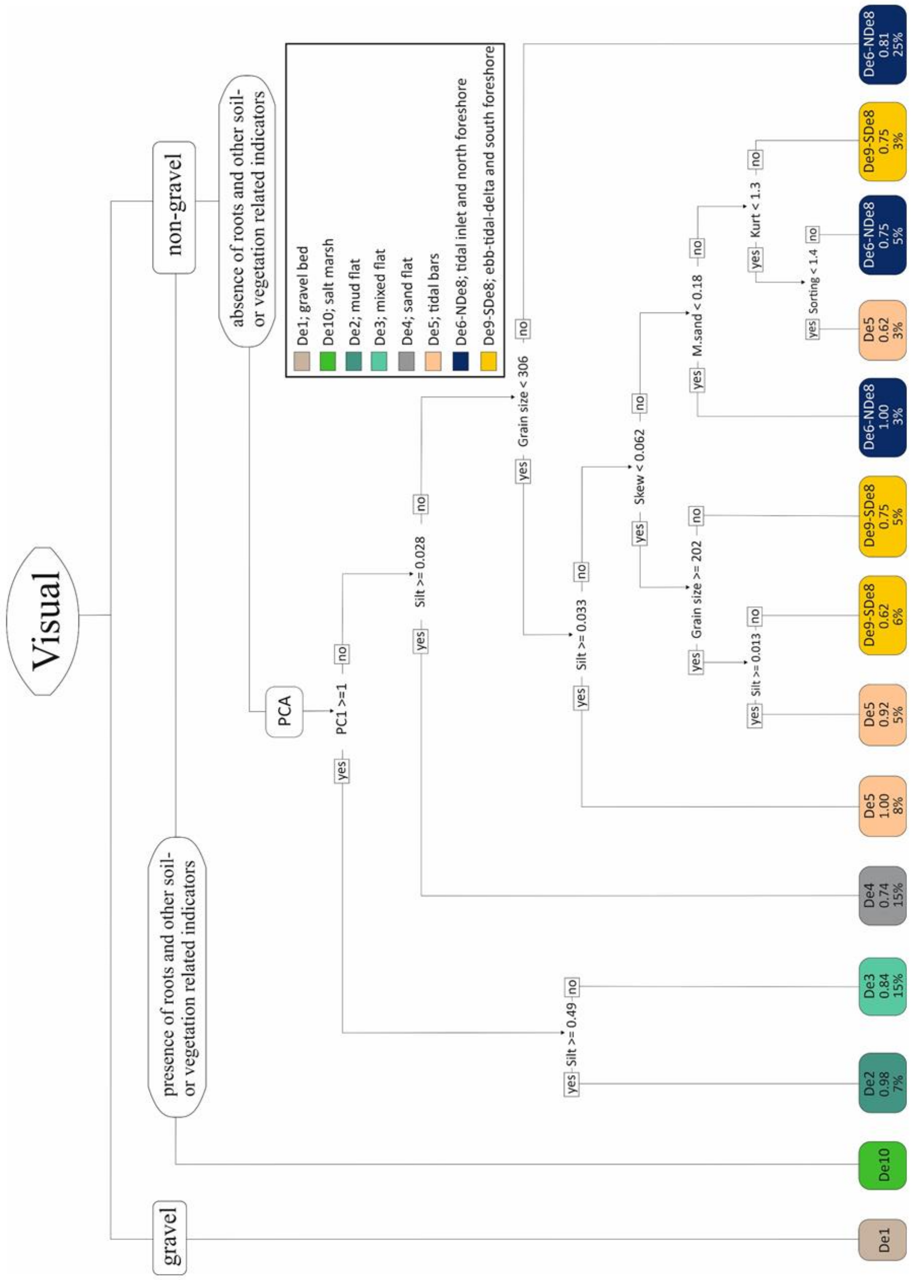

Figure 13 (please print this figure in landscape mode)

Figure 13; Discrimination diagram for the discrimination of depositional sub-environments, based on samples collected from the Ravenglass Estuary, developed through a combination of visual analysis (Fig. 3), differentiation of the principal component data and plus grain size, sorting, skew, kurtosis, medium sand fraction and silt fraction data (Figs. 10, 11, 12), using supervised classification and the recursive partitioning package, RPART (Therneau and Atkinson, 2019), available in R studio software (R Core Team, 2016). Each machine-learning-derived decision node splits the data using one data type. In each leaf (terminal) node, the classification (in this case, the depositional environment) is first listed.

The second value is the quantity of samples in that specific classification category, listed as a fractional quantity; high fractional quantities show that the classification has a high degree of certainty. Finally, the third value that RPART reports in the leaf nodes is the total percentage of the whole sample set that lies in each leaf node. This approach separated De2, De3 and De4 from De5 to De9 using the PCA output data plus the fractional quantity of silt. De5, De6-NDe8 and De9-SDe8 were subjected to RPART classification based on grain size, sorting, skew, kurtosis, silt fraction and medium sand fraction data. The pairs De6-NDe8 and De9-SDe8 were merged during feature engineering as the classification approach proved to be incapable of differentiating them. Each leaf (terminal) node lists the fraction of the samples in that specific classification category as a fractional quantity. Uncertainty, visible by fractional values less than 1.00, is the result of some samples falling in overlapping parts of multi-dimensional classification space, i.e., there are some categories (of depositional environments) that have overlapping attributes, even when four or six dimensions are considered.

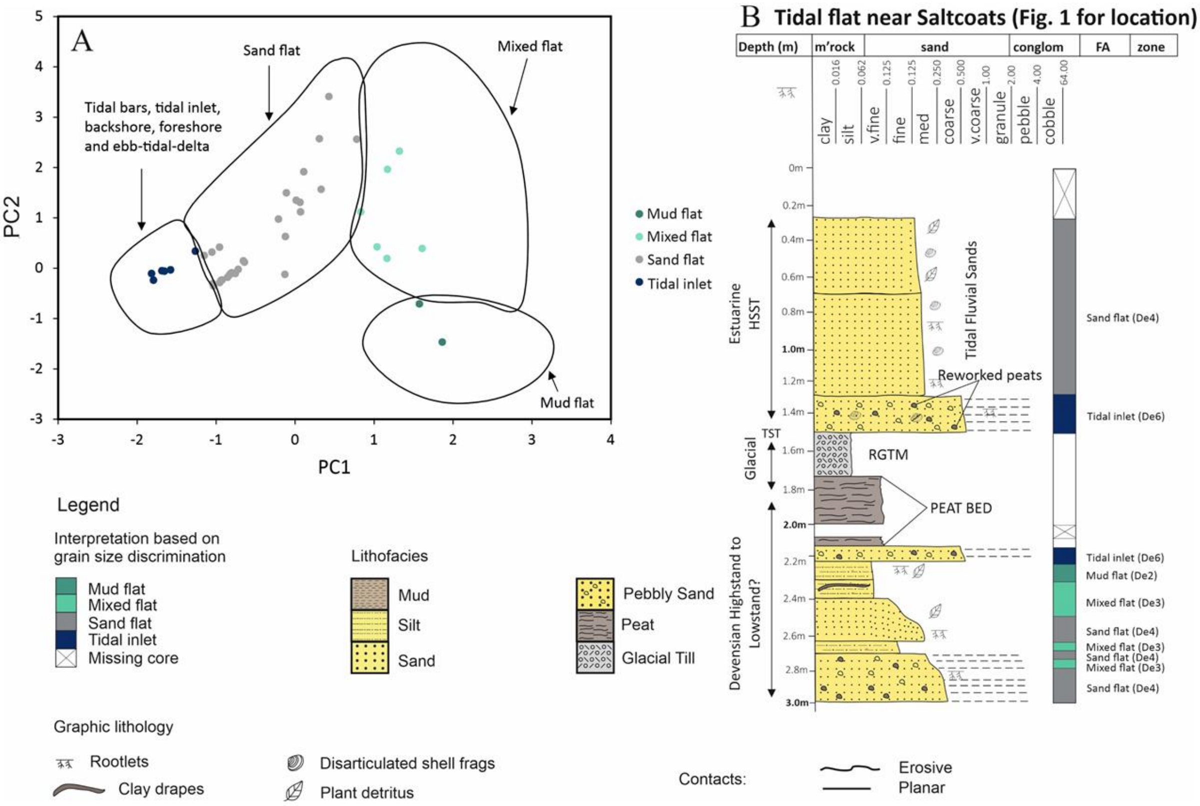

Figure 14

Figure 14. Schematic sedimentary log of central basin tidal flats deposits with application of the classification tree in Figure 13. A) Graphic log of a core from a sand flat in the central basin, near the hamlet of Saltcoats, with the sub-environments defined in the column to the right of the graphic log following application of the classification diagram (Fig. 13). B) Interpreted bivariate plot of replicated multivariate Principal Component Analysis (PCA) of samples from Holocene cores across Ravenglass Estuary, PC1 and PC2 discriminating loading score of each sampled, Ravenglass Estuary grain size data (mean grain size, sorting, skewness and kurtosis, phi unit). The replicated PCA shows the colour coded of each sampled within different sub-depositional environments.

Author and year	**Depositional environment**	**Method**	**Data interpretation method**
Flood et al. (2015)	Deltaic	LPSA	Compositional data analysis (CODA) associated with a multivariate statistical framework (PCA and Cluster analysis (CA))
Purkait and Majumdar (2014)	Deltaic	Sieving	Log-normal, log-skew-Laplace and discriminant analysis
Zubillaga and Edwards (2005)	Desert and coastal dunes	LPSA	Linear discriminant analysis and ANOVA
Friedman (1979)	Beach, inland and nearshore dune sands	Sieving	Bivariate analysis
Moiola and Spencer (1979)	Inland aeolian and coastal aeolian sands	Sieving	Discriminant analysis
Moiola et al. (1974)	Beach, coastal dune, inland dune, and fluvial	Sieving	Discriminant analysis
Greenwood (1969)	Marine and aeolian sands	Sieving	Linear discriminant analysis
Visher (1969)	Coastal	Sieving	Log-probability grain size distribution curves
Sevon (1966)	Fluvial, beach and aeolian sands	Sieving	Discriminant analysis
Klovan (1966)	Coastal	Sieving	Factor analysis
Biederman (1962)	Beach, dune, lagoon and marsh sediments	Sieving	Histogram and bivariate analysis
Friedman (1962)	Beach and river sands	Sieving	Bivariate analysis and mathematical computation
Friedman (1961)	Aeolian, beach and river sands	Sieving	Bivariate analysis
Shepard et al. (1961)	Aeolian and beach sands	Sieving/ microscopy	Bivariate analysis
Mason and Folk (1958)	Aeolian, beach and river sands	Sieving	Bivariate analysis
Keller (1945)	Aeolian and beach sands	Sieving	Ratio

Table 1

Eigenanalysis of the correlation matrix				
Eigenvalue	2.4762	1.1118	0.2794	0.1326
Proportion	0.6190	0.2780	0.0700	0.0330
Cumulative	0.6190	0.8970	0.9670	1.0000

Table 2

Eigenvectors				
Variable	PC1	PC2	PC3	PC4
Mean grain size	0.546	-0.348	-0.585	0.488
Grain size sorting	0.6	-0.158	-0.001	-0.784
Skewness	0.561	0.245	0.694	0.379
Kurtosis	0.165	0.891	-0.419	-0.053

Table 3

Depositional environment discrimination	Discriminatory variable	P-values	Useful for 1st order discrimination of sub-environments in this study
De6-De5	Grain size	0.0000015***	Y
N-De8-De5	Grain size	0.0000007***	Y
De9-De6	Grain size	0.0014742**	Y
S-De8-De6	Grain size	0.0000010***	Y
De9-N-De8	Grain size	0.0052703**	Y
S-De8-N-De8	Grain size	0.0000025***	Y
De6-De5	Medium sand fraction	0.0094279**	
N-De8-De5	Medium sand fraction	0.0029329**	
S-De8-De5	Medium sand fraction	0.0005359***	Y
S-De8-De6	Medium sand fraction	0.0000001***	
De9-S-De8	Medium sand fraction	0.0002193***	Y
S-De8-N-De8	Medium sand fraction	0.0000000***	
De9-De5	Kurtosis	0.0257901*	Y
N-De8-De5	Kurtosis	0.0115690*	
De6-De5	Sorting	0.0183192*	
De9-De5	Sorting	0.0186735*	
N-De8-De5	Sorting	0.0028333**	
De6-De5	Skewness	0.0274987*	
N-De8-De5	Skewness	0.0000049***	
S-De8-De5	Skewness	0.0293121*	

Table 4